# Elementary excitation spectrum of one-dimensional electron systems in confined semiconductor structures: Zero magnetic field

Q. P. Li* and S. Das Sarma
*Department of Physics and Astronomy, University of Maryland, College Park, Maryland 20742*
(Received 13 August 1990)

We study theoretically the elementary excitation spectrum in various one-dimensional electron systems in the absence of a magnetic field. We first calculate the elementary excitations in a single quantum wire under the random-phase approximation. We find that the intersubband collective excitation frequency can be 5–6.5 times higher than the corresponding single-particle excitation energy due to a large depolarization shift. Next, we calculate the plasmon excitation energy of a double-layered quantum-wire system. Our result shows that the resonance peak splits due to the Coulomb interaction between electrons in different layers. We also study the elementary excitations in one-dimensional lateral quantum-wire superlattices. We include the Coulomb interaction between electrons in different wires and allow tunneling between neighboring wires. Finally, we calculate the spectral weights of the elementary excitations of both a single quantum wire and quantum-wire superlattices for various parameter values. We compare our results with recent experiments and find good agreement.

## I. INTRODUCTION

Quasi-one-dimensional electron systems (1DES's, also called quantum wires) are usually fabricated on high-mobility two-dimensional (2D) electron systems[1] by adding an additional confinement along one of the remaining free directions using ultrafine lithographic techniques.[2–4] Recently, direct molecular-beam epitaxy (MBE) growth of 1DES's on GaAs-AlAs "tilted superlattices" has been reported.[5] The direct growth method is capable of growing samples with smaller wire widths than the lithographic method.

Undoubtedly, one of the motivations to study 1DES's is their obvious technological potential, such as achieving even higher mobilities than the two-dimensional electron gases (2DEG's) on which they are built. The reason for this is that in the low-energy regime (compared to the subband separation), the only relevant scattering mechanism in 1DES is back-scattering, which occurs relatively rarely. However, much more work needs to be done before this (i.e., reducing the scattering) can be experimentally realized because of imperfections on the boundary of the quantum wires. Apart from their technological potential, these 1D systems offer an excellent opportunity to experimentally study some of the fundamental concepts and methods of condensed-matter theory in a novel environment, for example, the electron localization problem (or electron transport in general). Now we understand that as the system size changes from larger than the electron phase-coherence length to smaller than the elastic-scattering length, the system goes through the universal-conductance-fluctuation region into the ballistic-transport region.[6,7] In the ballistic-transport region, Van Wees *et al.*[8] and Wharam *et al.*[9] independently, find quantization of the conductance of 1DES's without an external magnetic field. This is understood on the basis of the opening or closing of 1D subbands, which are also called "channels" as in the multichannel Landauer formula.[6,10,11] These kinds of phenomena associated with the 1DES's because of their small sizes (less than the mean-free path) and/or low dimensionalities make 1DES's a very interesting area of research. In the presence of an external magnetic field, there are more interesting phenomena arising in 1DES's. For example, in a magnetic field ($B$), a periodic array of quantum wires or a 1D lateral quantum-wire superlattice exhibits interesting oscillating features because of the competition (or commensurability) of the two length scales involved in the problem: the superlattice period $d$ and the Landau length $l=(\hbar c/eB)^{1/2}$. It has been found that in such superlattices the magnetoresistance shows oscillations periodic in $1/B$.[12–14] Magnetoplasmon oscillations have also been predicted in such systems.[15] A better understanding of elementary excitations of 1DES's in a magnetic field may also shed some light on the issue of edge states in the quantum-Hall effect.[16–18]

The density of states (DOS), defined as $dN/dE$, the number of states per unit energy, of a 1D quantum wire with finite width is given by ($\hbar=1$)

$$D(E)=(2/\pi)(m/2)^{1/2}\sum_{E_n<E}(E-E_n)^{-1/2}\,. \tag{1.1}$$

Here $E_n$ is the energy level due to the finite-width confinement of the quantum wire and $m$ is the effective mass of the electrons. When the 1D electron density $N_w$ is small enough and the temperature is low enough ($k_BT\ll E_2-E_1$), only the lowest subband is occupied, and Eq. (1) can be simplified as ($E_1=0$)

$$D(E)=(2/\pi)(m/2)^{1/2}E^{-1/2}\,. \tag{1.2}$$

It is quite clear that the DOS of a quantum wire is singu-

 

lar at $E=E_n$. In 3D and 2D electron systems, on the other hand, the DOS is proportional to $E^{1/2}$ and $E^0$, respectively, and is finite everywhere. Since many physical quantities are related to the DOS, we often need to deal with the singularity, and if necessary, choose a right cutoff in the theoretical model of 1DES's. In real systems, one expects disorder arising from random impurities in the system to have a smoothening effect on the singular $D(E)$ given by Eq. (1). Phenomenologically, the broadening can be characterized by a parameter $\gamma=\hbar/\tau$, where $\tau$ is the single-particle scattering time.[19]

In an ideal 1DES (zero width), the Fourier transformation of the Coulomb interaction

$$V(x,x')=\frac{e^2}{\epsilon|x-x'|} \tag{1.3}$$

is divergent. However, if we assume a more realistic finite-width model, the 1D Fourier transformation of the Coulomb interaction

$$V(\mathbf{r},\mathbf{r}')=\frac{e^2}{\epsilon[(x-x')^2+(y-y')^2]^{1/2}} \tag{1.4}$$

is given by[20,21]

$$v(q,y-y')=\frac{2e^2}{\epsilon}K_0(|q(y-y')|)\ . \tag{1.5}$$

Thus the matrix element of the Coulomb interaction

$$V_{ijmn}(q)=\int dy\int dy'\phi_i(y)\phi_j(y)v(q,y-y')\times\phi_m(y')\phi_n(y') \tag{1.6}$$

is finite for finite wave vector $q$. Here $\phi_i(y)$ is a confining wave function of the $i$th subband in the $y$ direction and $\epsilon$ is the background lattice dielectric constant. $K_0(x)$ is the zeroth-order modified Bessel function of the second kind, which diverges as -ln($x$) when $x$ goes to zero. Even in the limit of $q\rightarrow 0$, as we shall prove in Sec. II, some matrix elements of the Coulomb interaction such as $v_{1212}(q)$ are still finite, whereas others such as $v_{1111}(q)$ diverge as $\ln(qa)$. Here $a$ is the width of the quantum wire. Fortunately, this divergence is very weak (only logarithmic) and is not sensitive to the cutoff. Theoretically, while 1D systems have these additional difficulties as discussed above, they also have some simplifications compared to the 2D and 3D cases. Some 1D models, such as the 1D Hubbard model, are exactly soluble.[22,23] A nontrivial exact solution is valuable because it not only solves the problem in one dimension, but also helps us understand the properties and the structures of its higher-dimensional counterparts.

We point out that in 1D electron systems there is no Landau damping except on two isolated lines $E=E_q\pm qv_F$. Here $E_q=q^2/2m$, and $v_F=k_F/m$ is the Fermi velocity (we use $\hbar=1$ throughout this paper). This is quite different from the 2D and 3D cases, where there is a continuous Landau damping region $E_q-qv_F\leq E\leq E_q+qv_F$ in the energy-momentum space. Landau damping, as proposed by Landau,[24] is a damping mechanism in which a collective mode decays rapidly by exciting a single particle-hole pair. In general, once Landau damping becomes possible, the collective mode has such a short lifetime that it no longer represents a well-defined excitation of the system.[25] In 1D systems, the single particle-hole continuum of 2D and 3D systems becomes two isolated lines, and most of the collective excitations will not be Landau damped because the conservation of energy and the conservation of momentum cannot be satisfied simultaneously to allow the decay of a collective mode into a particle-hole pair in the region other than these two lines.

1D intersubband collective excitation has been observed by Hansen *et al.*[2] in a far-infrared spectroscopy experiment. Since then, 1DES's have been a very active research area.[3,20,21,26–34] In another 1DES experiment, Demel *et al.*[3] did both far-infrared spectroscopy and magnetoresistance measurements. They found a big discrepency between their optical and transport measurement data: at zero magnetic field, they found that the resonant frequency is 4 meV, while they also found that their magnetoresistance data could be best fitted by assuming the zero-field subband separation to be 1 meV. In this paper, we theoretically study the collective excitations in various kinds of 1DES's. Our calculations show that the experimental results can be explained by a very large depolarization shift in 1DES's.

We report our work in two papers: In this paper (paper I), we calculate the elementary excitation spectra of various kinds of semiconductor-based 1DES's in the zero magnetic field within the random-phase approximation (RPA) or the self-consistent-field approximation.[35] In another paper (paper II),[36] we will discuss the collective excitations of quantum wires in the presence of a magnetic field. Unless otherwise explicitly stated, all our discussions are for electrons in conduction subbands of $GaAs/Al_xGa_{1-x}As$ structures, even though most of the theory should be of general validity for any free-carrier system with isotropic and parabolic effective-mass band dispersion.

The rest of the paper is organized as follows. In Sec. II we calculate the collective excitations in a single quantum wire using multisubband models. We derive the dispersion relations for both intrasubband and intersubband excitations and discuss the mode-coupling effect between them. In Sec. III we calculate the collective excitations in a double-layer quantum-wire system. We devote Sec. IV to the discussion of collective excitations in multiwire and lateral quantum-wire superlattice systems. We include Coulomb interaction among different wires and allow tunneling between neighboring wires. In Sec. V we show our calculated results for the spectral weights of the collective ("charge-density") and the single-particle ("spin-density") excitations. We conclude the paper with some discussions, in Sec. VI. Some of our results appeared in brief communications[21,33] published earlier by us.

Equations in this paper are labeled by section and number, such as Eq. (2.15). When referenced within the same section, however, the section designation is usually dropped.

## II. ELEMENTARY EXCITATIONS IN A SINGLE QUANTUM WIRE

We assume the 2DEG to be confined in the $xy$ plane. We impose an additional confinement in the $y$ direction. Usually the confinement in the $z$ direction is much stronger than the confinement in the $y$ direction in real systems. In terms of energy scales, the energy-level separation is about a few meV in the $y$ direction, while in the $z$ direction it is of the order of $10^{-1}$ eV. In the low-energy regime, if the 2D electron density is not too high ($N_s < 5\times 10^{11}$ cm$^{-2}$), we can assume that the electrons are always in the lowest subband in the $z$ direction. For the sake of simplicity, we assume the 2DEG has zero thickness in the $z$ direction. Thus, the $z$ direction drops out of consideration, and the problem becomes a 2D problem in the $x$-$y$ plane. The generalized dielectric function $\epsilon_{ijmn}(q,\omega)$ for a single quantum wire is given by[21,37]

$$\epsilon_{ijmn}(q,\omega)=\delta_{im}\delta_{jn}-v_{ijmn}(q)\Pi_{mn}(q,\omega) , \tag{2.1}$$

where $i,j,m,m$ denote subbands because of confinement in the $y$ direction. $q$ is a 1D wave vector in the direction in which the motion is free. $\delta_{im}$ is the Kronecker $\delta$ function. The function $\Pi_{mn}(q,\omega)$ is a generalized 1D irreducible polarizability function. The subband matrix element of the Coulomb interaction $v_{ijlm}$ is given by Eq. (1.6). Note that Eq. (1) is a definition of a generalized dielectric function of any multi-component plasma; the index $i$, $j$, $m$, and $n$ could be spin index, layer index (see Sec. III), or as in our case, the subband index. In Sec. IV, we shall derive Eq. (1) from the linear-response theory [cf. Eq. (4.20)].

The collective excitation spectrum is obtained by the condition of the vanishing of the determinant of the dielectric matrix given in Eq. (1):

$$\det|\epsilon_{ijmn}|=0 . \tag{2.2}$$

To begin with, we restrict ourselves to a two-subband model in which only the lowest subband (denoted by 1) is occupied by electrons. Under this assumption, $\Pi_{22}(q,\omega)$ is zero at zero temperature, and is negligibly small at low temperatures. Thus Eq. (2) gives

$$(1-v_{1111}\Pi_{11})(1-v_{1212}\chi_{12})-v_{1112}^2\Pi_{11}\chi_{12}=0 , \tag{2.3}$$

where $\chi_{12}=\Pi_{12}+\Pi_{21}$ is the intersubband polarizability. Within the random-phase approximation one can use the noninteracting polarizability functions ("bare bubble") for $\Pi$'s in Eq. (3). The noninteracting 1D polarizability functions are given by

$$\Pi_{mn}(q,\omega)=2\int\frac{dp}{2\pi}\frac{n_F(\xi_p+E_n)-n_F(\xi_{p+q}+E_m)}{\omega+\xi_p+E_n-E_m-\xi_{p+q}} , \tag{2.4}$$

where $n_F(\xi_p+E_n)=\{\exp[\beta(\xi_p+E_n)]+1\}^{-1}$ is the Fermi distribution function, $\xi_p=p^2/2m-\mu$, $\mu$ is the chemical potential, and $\beta=1/k_BT$. At zero temperature, these $\Pi$'s are easily calculated to be

$$\Pi_{11}(q,\omega)=\frac{m}{\pi q}\ln\left[\frac{\omega^2-(E_q-qv_F)^2}{\omega^2-(E_q+qv_F)^2}\right] , \tag{2.5}$$

$$\chi_{12}(q,\omega)=\frac{m}{\pi q}\ln\left[\frac{\omega^2-(E_q-qv_F+E_{21})^2}{\omega^2-(E_q+qv_F+E_{21})^2}\right] , \tag{2.6}$$

where the subband separation $E_{21}=E_2-E_1$. In the long-wavelength limit, i.e., when $q\to 0$,

$$\Pi_{11}(q,\omega)=\frac{N_w}{m}\frac{q^2}{\omega^2}+O(q^4) , \tag{2.7}$$

$$\chi_{12}(q,\omega)=\frac{2E_{21}N_w}{\omega^2-E_{21}^2}+O(q) . \tag{2.8}$$

Here $N_w$ is the 1D density of electrons (i.e., the number of electrons per unit length). Notice that the long-wavelength forms of polarizability given by Eqs. (7) and (8) are independent of the dimensionality of the system, and have the same form as in Eqs. (7) and (8) for higher dimensions as well.[37]

The physical meaning of Eq. (3) is as follows. The zero of $(1-v_{1111}\Pi_{11})$ gives the intrasubband 1D plasmon excitation, which corresponds to the collective charge-density oscillations in the free $x$ direction, whereas $(1-v_{1212}\chi_{12})=0$ determines the 1D intersubband plasmon excitation, which corresponds to collective charge-density oscillations in the direction perpendicular to the quantum wire (along the $y$ direction in our case). These two modes are coupled by a term $-v_{1112}^2\Pi_{11}\chi_{12}$. Clearly, this intuitively appealing separation of the elementary excitation spectrum into distinct intrasubband and intersubband modes is strictly valid only when the coupling term is zero. When the coupling term is nonzero, the electric fields associated with the "longitudinal" and "transverse" motions couple, and the distinction between intrasubband and intersubband excitations is no longer strictly valid. However, we use the names intrasubband and intersubband excitations to label the two branches of solutions of Eq. (2.3) when the correction due to the coupling is small.

For a symmetric potential well, $v_{ijmn}(q)$ is strictly zero for arbitrary $q$ if $(i+j+m+n)$ is an odd number.[38] This is simply because the wave function is either symmetric or antisymmetric under space reflection. We assume the confining potential in the $y$ direction to be of a square-well form in our calculation.[21] Thus $v_{1112}$ is zero, and the mode-coupling term $-v_{1112}^2\Pi_{11}\chi_{12}$ vanishes. Equation (3) in this case becomes decoupled.

We first consider the intrasubband plasmon excitation ($\omega_p$), which is given by

$$1-V_{111}(q)\Pi_{11}(q,\omega_p)=0 . \tag{2.9}$$

We can solve Eq. (9) using Eq. (5) to get

$$\omega_p^2=[A(q)\omega_+^2-\omega_-^2]/[A(q)-1] , \tag{2.10}$$

where

$$A(q)=\exp[q\pi/mv_{1111}(q)] , \tag{2.11}$$

$$\omega_\pm=qv_F\pm q^2/2m . \tag{2.12}$$

In the long-wavelength limit $q \rightarrow 0$, we can simplify Eq. (10) as

$$\omega_p = qa\omega_0 |\ln(qa)|^{1/2} + O(q^2) , \tag{2.13}$$

where $\omega_0 = (2N_w e^2/\epsilon m a^2)^{1/2}$ and $a$ is the width of the quantum wire. We notice that $a$ appears in the zeroth-order term, unlike in the 2D plasmon case, in which the finite-width effects appear only in higher-order terms[20] of the expansion.

Next we consider the intersubband collective excitation

$$1 - v_{1212}(q)\chi_{12}(q,\omega) = 0 . \tag{2.14}$$

We can solve Eq. (14) using Eq. (6):

$$\omega^2 = [B(q)\Omega_+^2 - \Omega_-^2]/[B(q)-1] , \tag{2.15}$$

where

$$B(q) = \exp[q\pi/m v_{1212}(q)] , \tag{2.16}$$

$$\Omega_\pm = E_{21} \pm q v_F + q^2/2m . \tag{2.17}$$

In the long-wavelength limit $q \rightarrow 0$, we can simplify (15) as

$$\begin{aligned} \omega^2 &= E_{21}^2 + 2E_{21} N_w v_{1212}(q \rightarrow 0) + O(q) , \\ &= E_{21}^2 + W_P^2 + O(q) , \end{aligned} \tag{2.18}$$

where $W_P = [2E_{21} N_w v_{1212}(q \rightarrow 0)]^{1/2}$ is the so-called depolarization shift,[1,39] which measures the energy difference between the intersubband single-particle and collective excitations. $v_{1212}(q \rightarrow 0)$ is about $1.2e^2/\epsilon$ for a square-well potential. It is easy to understand why $v_{1212}(q \rightarrow 0)$ is finite, while $v_{1111}(q \rightarrow 0)$ diverges as $|\ln(qa)|$ using the asymptotic expansion of the Bessel function $K_0(x)$and the orthogonality of the wave functions. When $q \rightarrow 0$,

$$K_0(|q(y-y')|) \simeq -\ln(qa) - \ln|(y-y')/a| . \tag{2.19}$$

From Eq. (1.6) it is quite clear that the first term of Eq. (19) $-\ln(qa)$ contributes to the divergence of $v_{1111}(q \rightarrow 0)$ but not to $v_{1212}(q \rightarrow 0)$ due to orthogonality of the wave functions. The contribution of the second term $-\ln|(y-y')/a|$ is always finite and does not depend on $q$.

The intersubband single-particle excitation frequency is given by

$$\chi_{12}^{-1}(q,\omega) = 0 . \tag{2.20}$$

In Fig. 1 we show the calculated dispersion of the intersubband collective excitation between the first and second subbands and the corresponding single-particle excitation within the two-subband model. One can see that for $q = 0$ the collective excitation frequency is about six times as high as that of the single-particle excitation. This is in qualitative agreement with the experimental result of Demel *et al.*[3] To characterize this large enhancement due to the many-body effect, we introduce a parameter

$$\gamma_{12}(q) = \omega_{12}^c(q)/\omega_{12}^s(q) \tag{2.21}$$

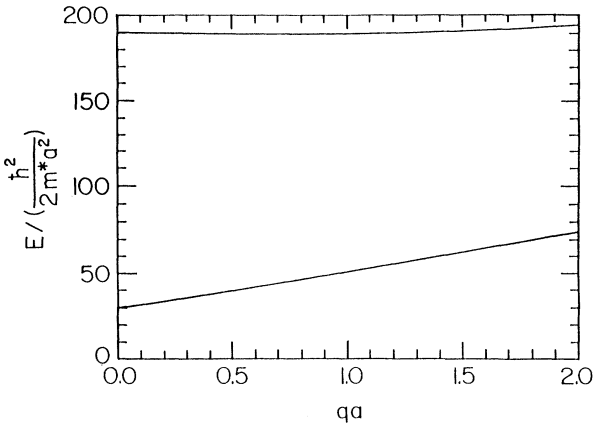


FIG. 1. The intersubband single-particle excitation (lower branch) and the intersubband collective excitation (upper branch) between subbands 1 and 2 as a function of $qa$ in a two-subband model. (The parameters $a = 390$ nm, $N_w = 0.166 \times 10^6$ cm$^{-1}$ are chosen according to Ref. 3).

as the ratio of the intersubband collective excitation and the single-particle excitation frequency. $\gamma_{12}(q=0)$ is about 6.3 in our two subband model. The parameters used in our calculation are in accordance with the experiment of Demel *et al.*[3] (sample *A*) with the difference that $N_w$ is scaled down for our calculation from the experimental total electron density by a factor

$$\frac{N_{w1}}{N_{w12}} = \frac{(E_{F1} - E_1)^{1/2}}{\sum_{n=1}^{12} (E_{F12} - E_n)^{1/2}} , \tag{2.22}$$

which takes into account the fact that the experimental sample has 12 subbands occupied, whereas in our model calculation only one subband is assumed to be populated. $E_n = n^2\pi^2/2ma^2$ is the energy bottom of the $n$th subband, and $E_F$ is the Fermi energy. We further assume that the Fermi energy $E_{F1}$ ($E_{F12}$) is at the bottom of the second (thirteenth) subband. Because the generalized dielectric-function matrix has dimensions $B^2 \times B^2$, where $B$ is the number of subbands in the model, it is very difficult to calculate the elementary excitation spectrum for a thirteen-subband model using our method. Thus the semiquantitative comparison between theory and experiment as carried out here is the best one can do at this stage. Next we shall extend our calculation to a three-subband model, which exhibits some interesting features not found in the two-subband calculation described above. In particular, a mode coupling between the intrasubband and intersubband excitations shows up in the three-subband model. We also discuss the intersubband collective excitation and single-particle excitation between the second and third subbands. The agreement between theory and experiment improves in this three-subband calculation, lending further support to our model.

In the three-subband model, we assume that only the two lowest subbands are occupied (denoted by 1 and 2). Under this assumption, $\Pi_{33}(q,\omega)$ is zero. This reduces Eq. (2) to an $8\times8$ determinant. Using the symmetry of the potential well, the $8\times8$ determinant can be decoupled to two $4\times4$ determinants, which can be further reduced to the following two equations, after some algebra:

$$(1-v_{1212}\chi_{12})(1-v_{2323}\chi_{23})-v_{2321}^2\chi_{12}\chi_{23}=0 \tag{2.23}$$

and

$$(1-v_{1313}\chi_{13})[(1-v_{1111}\Pi_{11})(1-v_{2222}\Pi_{22})-v_{1122}^2\Pi_{11}\Pi_{22}]-2v_{1122}v_{1113}v_{2213}\Pi_{11}\Pi_{22}\chi_{13}$$
$$-(1-v_{1111}\Pi_{11})v_{2213}^2\Pi_{22}\chi_{13}-(1-v_{2222}\Pi_{22})v_{1113}^2\Pi_{11}\chi_{13}=0\ , \tag{2.24}$$

where $\chi_{13}=\Pi_{13}+\Pi_{31}$ is the intersubband polarizability.

Clearly, Eq. (23) corresponds to the mode coupling between intersubband collective excitations of subbands 1 and 2 and that of subbands 2 and 3. Equation (24) is more complicated, describing the coupling among the intersubband collective excitation of subbands 1 and 3 and the two intrasubband plasma excitations of subbands 1 and 2. We start with Eq. (23), which we believe includes the relevant physics needed to explain the experimental results of Demel *et al.*[3] First we calculate the intersubband collective excitation $\omega_{23}^c(q)$ of subbands 2 and 3, which is determined by

$$1-v_{2323}(q)\chi_{23}(q,\omega)=0\ . \tag{2.25}$$

In the three-subband model, $\gamma_{23}(q=0)$ is about 5.4, which is smaller than $\gamma_{12}(q=0)=6.3$ in our two-subband model and closer to the experimental result $\gamma=4.0$. In Fig. 2 we show the numerical solution $\Omega(q)$ of Eq. (23) as a function of $qa$. The uncoupled intersubband collective excitation modes $\omega_{23}^c$ and single-particle excitation $\omega_{23}^s$ are also plotted in the figure for comparison. After mode coupling, the collective excitation is about 1.3% above $\omega_{23}^c$ at $q=0$. We can see that the correction due to the coupling is rather small. The reason is that $\chi_{12}$ is much smaller than $\chi_{23}$ in the three-subband model as the result of our assumption that subbands 1 and 2 are occupied while subband 3 is empty. Thus, in the coupling term of Eq. (23), $\omega_{12}$ has a small correction on $\omega_{23}$, while $\omega_{23}$ has a large effect on $\omega_{12}$, so large, in fact, that the other branch of the coupled solution corresponding to $\omega_{12}$ does not exist anymore.

Next we consider Eq. (24). In Fig. 3 we show the coupling between the intrasubband plasma excitations of subbands 1 and 2:

$$(1-v_{1111}\Pi_{11})(1-v_{2222}\Pi_{22})-v_{1122}^2\Pi_{11}\Pi_{22}=0\ . \tag{2.26}$$

The uncoupled plasma modes $\omega_{11}$ and $\omega_{22}$ in each subband are also plotted for comparison. In Fig. 4 we plot the three branches of the solution of Eq. (24). Apparently, the highest branch corresponds to the intersubband collective excitation $\omega_{13}$, while the two lower branches correspond to the coupled intrasubband plasmon excitations (cf. Fig. 3).

In summary, we calculate the elementary excitation spectrum of a quasi-1D quantum wire within the two- and three-subband models and using the RPA for the dielectric response. We find that the intersubband collective excitation energy can be significantly higher than the corresponding single-particle excitation energy for exper-

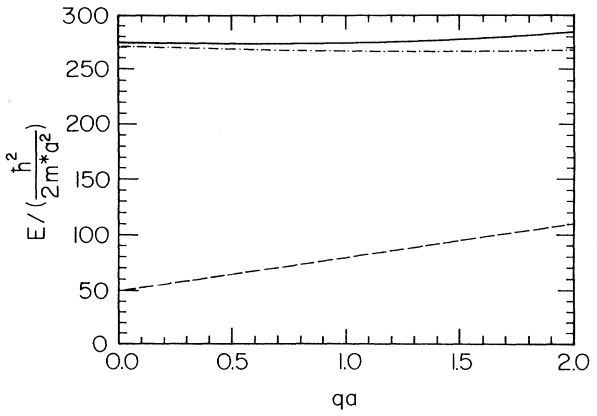


FIG. 2. The intersubband excitation between subbands 2 and 3 as a function of $qa$ in a three-subband model ($a=390$ nm, $N_w=0.486\times10^6$ cm$^{-1}$). The solid line is for $\Omega(q)$, the solution of the coupled Eq. (2.23), whereas the dashed line and the dotted-dashed line are for the uncoupled single-particle and collective excitations, respectively. The coupling effect pushes the other branch of $\Omega(q)$ below the abscissa in the figure.

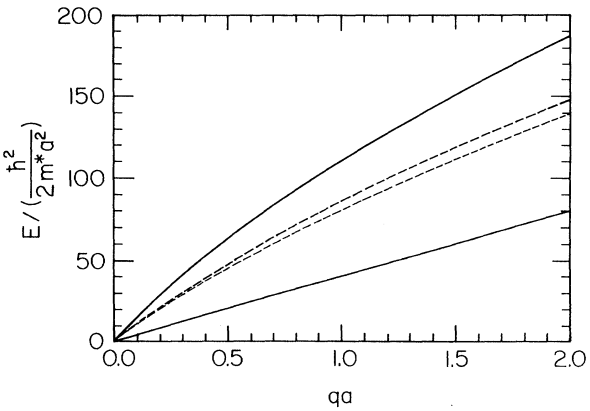


FIG. 3. The coupling between intrasubband plasmon excitations as a function of $qa$ in the same system as in Fig. 2. The solid lines are for the coupled modes and the dashed lines are for the uncoupled individual plasmon excitations of subbands 1 and 2, respectively.

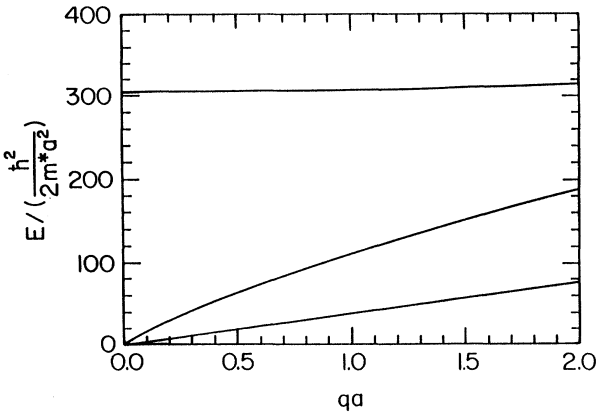


FIG. 4. The solution of Eq. (2.24), which describes the coupling between the intersubband collective excitation ($1\rightarrow 3$) and the intrasubband plasmon excitations of subbands 1 and 2. The system is the same as in Fig. 2.

imentally realizable parameter values. Our calculation shows that the ratio of the two energies can be as high as 5–6.5 using the experimental parameters adopted from Ref. 3. This is in good qualitative and semiquantitative agreement with experimental results.[3] We identify the experimentally observed infrared absorption peak to be the intersubband collective excitation mode. This identification is supported by the fact that in the zero magnetic field, the absorption peak was observed only when the incident light was polarized in the direction perpendicular to the 1D quantum wire, but not when it was parallel.

## III. COLLECTIVE EXCITATIONS IN A DOUBLE-LAYERED QUANTUM-WIRE SYSTEM

In their experiment, Demel *et al.*[3] also studied the far-infrared absorption spectrum of a double-layered quantum-wire system prepared by deep-mesa etching (sample *B*). They found that the absorption peak split into two peaks in the double-layered system. In this section, we calculate the collective excitations in a double-layered quantum-wire system and show that the splitting is due to the Coulomb interaction between the electrons in the different layers.

We assume that the electrons are confined in two zero-thickness planes $\delta(z)$ and $\delta(z-\Delta z)$ with a distance $\Delta z$ apart and that there is no tunneling between different layers. Additional confinement is induced along the $y$ direction. Thus we can define the generalized dielectric function:

$$\epsilon_{ijlm,\alpha\beta}=\delta_{il}\delta_{jm}\delta_{\alpha\beta}-V_{ijlm,\alpha\beta}\Pi_{lm,\beta} . \tag{3.1}$$

Here $i,j,l,m$ are the subband indices due to the $y$-direction confinement and $\alpha,\beta$ are the layer indices. $\Pi_{lm,\beta}$ is the generalized polarizability, and $V_{ijlm,\alpha\beta}$ is the matrix element of Coulomb interaction,

$$V_{ijlm,\alpha\beta}=V_{ijlm}\delta_{\alpha\beta}+(1-\delta_{\alpha\beta})U_{ijlm} , \tag{3.2}$$

where

$$V_{ijlm}(q)=\frac{2e^2}{\epsilon}\int dy\int dy'\phi_i(y)\phi_j(y)K_0(|q(y-y')|)\times\phi_l(y')\phi_m(y') \tag{3.3a}$$

is the matrix element of Coulomb interaction of electrons in the same layer, and

$$U_{ijlm}(q)=\frac{2e^2}{\epsilon}\int dy\int dy'\phi_i(y)\phi_j(y)\times K_0(q[(y-y')^2+(\Delta z)^2]^{1/2})\times\phi_l(y')\phi_m(y') \tag{3.3b}$$

is the matrix element of Coulomb interaction of electrons in the different layers.

The collective excitations of the system are given by the zeros of the generalized dielectric function.

$$\det|\epsilon_{ijlm,\alpha\beta}|=0 . \tag{3.4}$$

We assume a two-subband model, considering only the lowest two subbands, and assume that only the lowest subband (denoted by 1) is occupied by the electrons. Under this assumption, the generalized dielectric function is an $8\times 8$ matrix (it would be $16\times 16$ if we allowed tunneling between the two layers), and $\Pi_{22,\beta}(q,\omega)$ is zero at zero temperature. We further assume the confining potential in the $y$ direction to be symmetric. After some manipulation, Eq. (4) can be simplified and written as

$$1-[V_{1111}(q)\pm U_{1111}(q)]\Pi_{11}(q,\omega)=0 , \tag{3.5}$$

$$1-[V_{1212}(q)\pm U_{1212}(q)]\chi_{12}(q,\omega)=0 , \tag{3.6}$$

where $\chi_{12}=\Pi_{12}+\Pi_{21}$ is the intersubband polarizability function given by Eq. (2.6), and $\Pi_{11}$ the intrasubband polarizability function given by Eq. (2.5).

Equation (5) describes the splitting of the 1D intrasubband plasmon excitations due to the Coulomb interaction between the electrons in the two different layers. It is similar to what Das Sarma and Madhukar found for the 2D plasmon excitations in a double-layered quantum-well system.[40] Equation (6) describes the splitting of the intersubband plasmon excitations in the nontunneling double-layered quantum-wire system. The plus (minus) sign in Eqs. (5) and (6) corresponds to the collective mode in which electrons in the different layers are oscillating in (out of) phase.

We can solve Eq. (5) in a similar way to solving Eq. (2.9):

$$\omega_{p\pm}^2=[A_\pm(q)\omega_+^2-\omega_-^2]/[A_\pm(q)-1] , \tag{3.7a}$$

where

$$A_\pm(q)=\exp\{q\pi/m\,[V_{1111}(q)\pm U_{1212}(q)]\} , \tag{3.7b}$$

$$\omega_\pm=qv_F\pm q^2/2m . \tag{3.7c}$$

In the long-wavelength limit $q\rightarrow 0$, we can simplify Eq. (7a) as

$$\omega_{p\pm}^2=(N_w/m)q^2(V_{1111}\pm U_{1111})_{q\rightarrow 0}+O(q^4) . \tag{3.8}$$

Substituting Eq. (2.19) into Eq. (3) as $q\rightarrow 0$, we get that

$(V_{1111}+U_{1111})_{q\to 0}$ diverges as $-\ln(qa)$, while $(V_{1111}-U_{1111})_{q\to 0}$ is finite. So the 1D optical plasmon frequency (plus sign) behaves as $q|\ln(qa)|^{1/2}$ as $q\to 0$, whereas the acoustic plasmon frequency (minus sign) depends on $q$ linearly in the long-wavelength limit. It is interesting to compare this result with the 2D plasmon excitation energy in a double-layered quantum-well system as discussed by Das Sarma and Madhukar.[40] They found that the 2D optical plasmon frequency goes to zero as $q^{1/2}$ when $q\to 0$, therefore always staying outside the Landau damping region in the long-wavelength limit, whereas the acoustic plasmon is Landau damped when the distance between the two layers is smaller than a critical value $d_c$, and is undamped when the distance exceeds $d_c$.

As we discussed in the Introduction, in one-dimensional systems there is no Landau damping except on two isolated lines. This is quite different from the 2D and 3D cases, where we have a continuous Landau damping region. So in double-layered quantum-wire systems, both the optical and accoustic plasmons should be undamped observable modes.

The intersubband collective excitation in the double-layered quantum-wire system, Eq. (6), can be solved to give

$$\omega_{\pm}^2=[B_{\pm}(q)\Omega_{+}^2-\Omega_{-}^2]/[B_{\pm}(q)-1]\ , \tag{3.9a}$$

where

$$B_{\pm}(q)=\exp\{q\pi/m\,[V_{1212}(q)\pm U_{1212}(q)]\}\ , \tag{3.9b}$$

$$\Omega_{\pm}=E_{21}\pm qv_F+q^2/2m\ . \tag{3.9c}$$

In the long-wavelength limit $q\to 0$, we can simplify Eq. (9a) as

$$\omega_{\pm}^2=E_{21}^2+2E_{21}N_w[V_{1212}(q\to 0)\pm U_{1212}(q\to 0)]+O(q)\ . \tag{3.10}$$

In Fig. 5(a) we show the two branches of the intersubband collective excitation energy as a function of $qa$ for a double-layered quantum-wire system with $a=320$ nm, $\Delta z=130$ nm, and $N_w=0.135\times 10^6$ cm$^{-1}$. The single-particle excitation energy is also plotted for comparison. In Fig. 5(b) we plot $V_{1212}$ and $U_{1212}$ as a function of $qa$ for the same system. Apparently, the splitting of the plasma energy depends strongly on the separation $\Delta z$ between the two layers.

## IV. ELEMENTARY EXCITATIONS IN 1D LATERAL-QUANTUM-WIRE SUPERLATTICES

In Sec. II we discussed elementary excitations in a single quantum wire. Theoretically, it is relatively easy to deal with a single wire, which gives us insight into the understanding of the elementary excitation spectra in 1DES's. However, in order to get a satisfactory signal-versus-noise ratio, experimentalists usually like to work on a periodic array of 1D quantum wires or so-called 1D lateral superlattices.[2,3] Accordingly, we now consider elementary excitations in a multiwire electron system.

According to the strength of the tunneling between the neighboring quantum wires, two different approaches are adopted in calculating the elementary excitation spectra of such multiple-quantum-wire 1D superlattices. In the strong-tunneling limit, the system could be regarded as a 2D electron gas with a periodic modulation potential along one of its two directions. The modulation potential, if not too strong, can be treated as a perturbation.[14] In the weak-tunneling limit, on the other hand, the system can be treated as a periodic array of tight-binding quantum wires interacting with each other through Coulomb interaction with some small wave-function overlap.[33]

In this section we study the weak-tunneling 1D superlattice, which is intermediate between a 1D quantum wire (Sec. II) and a modulated 2D system referred to above. We derive a formalism for calculating the collective excitations of a 1D superlattice, including the mode coupling between the intrasubband and intersubband excitations from the linear-response theory[41,42] within the self-consistent-field approximation.[35] We also discuss how

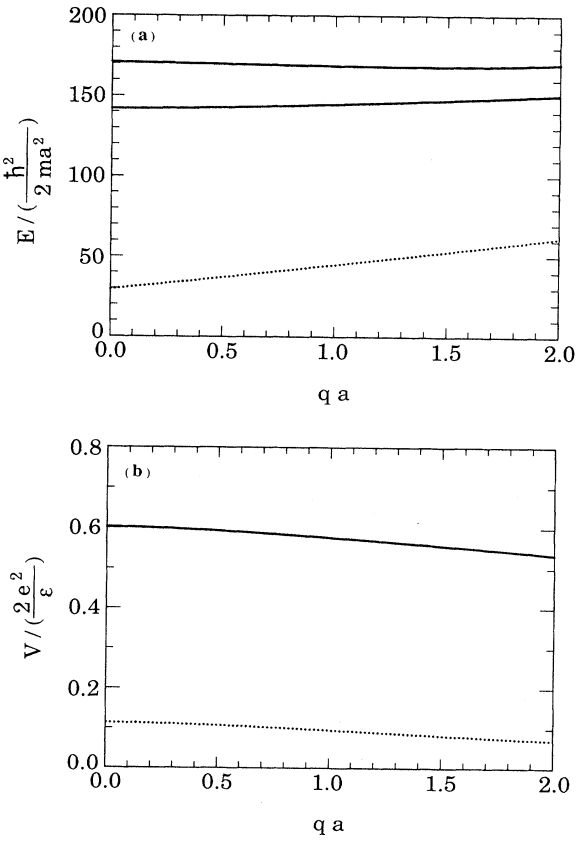


FIG. 5. (a) The two branches of the intersubband collective excitation energy as a function of $qa$ for a double-layered quantum-wire system with $a=320$ nm, $\Delta z=130$ nm, and $N_w=0.135\times 10^6$ cm$^{-1}$ The single-particle excitation energy (dotted line) is also plotted for comparison. (b) The matrix elements of Coulomb interaction between the electrons in the same and different layers, $V_{1212}$ (solid line) and $U_{1212}$ (dotted line), respectively, as a function of $qa$ for the same system.

quantum tunneling between neighboring wires modifies the plasmon dispersion.

As in Sec. II, we assume that electrons are confined in a zero-thickness $x$-$y$ plane for the sake of simplicity. We choose the $x$ direction to be the free direction. A periodic tight-binding-type confinement is imposed on the $y$ direction. The wave function and the energy of the system are

$$\psi(x,y,z)=(\tfrac{1}{2}\pi)^{1/2}\exp(ik_x x)\phi_{nk_y}(y)[\delta(z)]^{1/2} , \tag{4.1}$$

$$E_n(k_x,k_y)=k_x^2/2m+E_n+(\Delta_n/2)[1-\cos(k_y d)] , \tag{4.2}$$

with

$$\phi_{nk_y}(y)=N^{-1/2}R_{nk_y}\sum_{l=1}^{N}\exp(ik_y ld)u_n(y-ld) . \tag{4.3}$$

Here $n$ is the quantum subband index for the $y$ confinement and $d$ is the superlattice period. $N$ is the total number of wires, and

$$R_{nk_y}=[1+2\alpha_n\cos(k_y d)]^{1/2} \tag{4.4}$$

is the normalization factor. $\alpha_n$ is the overlap parameter characterizing our tight-binding model,

$$\alpha_n=\int_{-\infty}^{\infty}dy\, u_n(y)u_n(y-d) . \tag{4.5}$$

We assume the periodic confining potential is a finite square well (Kronig-Penney potential) with barrier height $V_0$ and well width $a$. In the tight-binding limit, the bandwidth $\Delta_n$ is given by

$$\Delta_n=4\int_{-a/2}^{a/2}dy\, u_n(y)V_0 u_n(y-d) . \tag{4.6}$$

To obtain the collective excitations of the 1D superlattice system described by above equations, we start with a standard linear-response theory.[41,42] We consider $\delta n(\mathbf{r})$, the deviation of the electron density from its equilibrium value, which can be related to the perturbation $V$ by

$$\delta n(\mathbf{r})=\sum_{a,b}\frac{f_b-f_a}{E_b-E_a+\omega}V_{ab}\psi_b^*(\mathbf{r})\psi_a(\mathbf{r}) , \tag{4.7}$$

where $a$ and $b$ are the composite quantum indices, $f_b$ and $f_a$ are the Fermi distribution functions $n_F(E_a)$ and $n_F(E_b)$ [cf. Eq. (2.4)], and $V_{ab}$ are the matrix elements of the perturbing potential. For the system under consideration, we write Eq. (7) as

$$\delta n(q_x,\omega,y)=\sum_{n,m}\sum_{k_y,q_y}\Pi_{nm}(q_x,\omega,k_y,q_y)\times\langle nk_y|V|mk_y+q_y\rangle\times\phi^*_{mk_y+q_y}(y)\phi_{nk_y}(y) , \tag{4.8a}$$

where

$$\Pi_{nm}(q_x,\omega,k_y,q_y)=2\sum_{k_x}\frac{f_{m\mathbf{k}+\mathbf{q}}-f_{n\mathbf{k}}}{E_{m\mathbf{k}+\mathbf{q}}-E_{n\mathbf{k}}+\omega} \tag{4.8b}$$

where $\mathbf{k}=(k_x,k_y)$ and $\mathbf{q}=(q_x,q_y)$ are two-dimensional momenta. If we neglect the exchange term, the potential $V$ can be written as the sum of two parts, the external potential and Hartree potential:

$$V=V^{\rm ex}+V^H , \tag{4.9a}$$

where

$$V^H(\mathbf{r})=\int d\mathbf{r}'\frac{e^2}{\epsilon|\mathbf{r}-\mathbf{r}'|}\delta n(\mathbf{r}') . \tag{4.9b}$$

For the convenience of the calculation, we choose to work on a finite system and use the periodic-boundary condition in the $y$ direction,[43]

$$V^H(\mathbf{r})=\int d\mathbf{r}'\sum_t\frac{e^2}{\epsilon[(x-x')^2+(y-y'+tL)^2]^{1/2}}\times\delta n(\mathbf{r}') , \tag{4.10}$$

where the summation is over all integers $t$, $L$ is the size of the system in the $y$ direction, and $\epsilon$ the dielectric constant of the background lattice. From Eqs. (8), (9), and (10) we get

$$\langle nk_y|V^H|mk_y+q_y\rangle=\sum_{n',m'}\sum_{k_y',q_y'}\Pi_{n'm'}(q_x,\omega,k_y',q_y')u_{nmn'm'}(q_x,k_y,q_y,k_y',q_y')\langle n'k_y'|V^{\rm ex}+V^H|m'k_y'+q_y'\rangle , \tag{4.11}$$

where

$$U_{nmn'm'}(q_x,k_y,q_y,k_y',q_y')=\frac{2e^2}{\epsilon}\int_0^L dy\int_0^L dy'\phi_{mk_y+q_y}(y)\phi^*_{nk_y}(y)\sum_t K_0(|q_x(y-y'+tL)|)\phi^*_{m'k_y'+q_y'}(y')\phi_{n'k_y'}(y') . \tag{4.12}$$

The condition for collective excitations of the system is that self-sustaining oscillations in the electron density occur. This means that Eq. (11) has a nonzero solution $V^H$ when the external perturbation $V^{\rm ex}$ is zero.

### A. Isolated superlattice

First we consider the case of isolated superlattices, where there is no overlap between neighboring wave functions. In this case we have the following simplifications:

$$\phi_{nk_y}(y)=N^{-1/2}\sum_{l=1}^{N}\exp(ik_y ld)u_n(y-ld) , \tag{4.13}$$

$$E_n(k_y)=E_n \ , \tag{4.14}$$

$$\Pi_{nm}(q_x,\omega,k_y,q_y)=\Pi_{nm}(q_x,\omega) \ . \tag{4.15}$$

From Eqs. (12) and (13) we can easily show that for isolated superlattices

$$U_{nmn'm'}(q_x,k_y,q_y,k_y',q_y')=U_{nmn'm'}(q_x,q_y,q_y')$$
$$=\frac{2e^2}{\epsilon N^2}\int_0^L dy\int_0^L dy'\sum_l\sum_{l'}e^{iq_y ld}e^{-iq_y'l'd}u_n^*(y)u_m(y)$$
$$\times\sum_t K_0(|q_x[y-y'+(l-l')d+tl]|)u_{n'}(y')u_{m'}^*(y') \ . \tag{4.16}$$

We expand the Bessel function $K_0$ in Fourier space,

$$\sum_t K_0(|q_x(y-y'+tL)|)=(\pi/L)\sum_s\sum_{p_y=-\pi/d}^{\pi/d}\frac{\exp[i(p_y+s2\pi/d)(y-y')]}{[q_x^2+(p_y+s2\pi/d)^2]^{1/2}} \ , \tag{4.17}$$

where the summation over $s$ is over all integers. Using Eq. (17) we can, after some algebra, simplify Eq. (16):

$$U_{nmn'm'}(q_x,q_y,q_y')=\frac{2\pi e^2}{\epsilon L}\delta_{q_y,q_y'}\int dy\int dy'u_n^*(y)u_m(y)S(\mathbf{q},y-y')u_{n'}(y')u_{m'}^*(y') \ , \tag{4.18}$$

where

$$S(\mathbf{q},y-y')=\sum_s\frac{\exp[-i(q_y+s2\pi/d)(y-y')]}{[q_x^2+(q_y+s2\pi/d)^2]^{1/2}} \ . \tag{4.19}$$

From Eqs. (11), (15), and (18) we get the generalized dielectric function,

$$\epsilon_{nmn'm'}(q_x,q_y,\omega)=\delta_{nn'}\delta_{mm'}-\Pi_{nm}(q_x,\omega)v_{nmn'm'}(q_x,q_y) \ , \tag{4.20}$$

where

$$v_{nmn'm'}(q_x,q_y)=\frac{2\pi e^2}{\epsilon d}\int dy\int dy'u_n^*(y)u_m(y)S(\mathbf{q},y-y')u_{n'}(y')u_{m'}^*(y') \ . \tag{4.21}$$

Once we have the generalized dielectric function, the plasmon excitation spectrum is obtained by the condition of its determinant to be zero. If we restrict ourselves to a two-subband model in which only the lowest subband (denoted by 1) is occupied by electrons, we get

$$(1-v_{1111}\Pi_{11})(1-v_{1212}\chi_{12})-v_{1211}v_{1112}\Pi_{11}\chi_{12}=0 \ , \tag{4.22}$$

where $\chi_{12}=\Pi_{12}+\Pi_{21}$ is the intersubband polarizability. $\Pi_{11}$ and $\chi_{12}$ at zero temperature can be easily calculated using Eq. (8b),

$$\Pi_{11}(q_x,\omega)=\frac{m}{\pi q_x}\ln\left[\frac{\omega^2-(E_q-q_xv_F)^2}{\omega^2-(E_q+q_xv_F)^2}\right] \ , \tag{4.23}$$

$$\chi_{12}(q_x,\omega)=\frac{m}{\pi q_x}\ln\left[\frac{\omega^2-(E_{21}-q_xv_F+E_q)^2}{\omega^2-(E_{21}+q_xv_F+E_q)^2}\right] \ , \tag{4.24}$$

where $E_{21}=E_2-E_1$ is the subband separation, and $E_q\equiv q_x^2/2m$.

When $q_y$ is zero, $v_{1112}$ and $v_{1211}$ are zero because of the even symmetry of the confining potential, decoupling the intrasubband and intersubband excitations. For nonzero $q_y$, the symmetry is broken and $v_{1112}=v_{1211}^*$ becomes nonzero, and therefore the intrasubband and intersubband plasmon excitations are coupled according to Eq. (22). Thus, within this model, mode coupling exists only for $q_y\neq 0$

If we neglect the coupling term, the intrasubband plasmon excitation of an isolated 1*D* superlattice is given by

$$1-v_{1111}(\mathbf{q})\Pi_{11}(\mathbf{q},\omega)=0 \ , \tag{4.25}$$

where $v_{1111}(\mathbf{q})$ is given by Eq. (21). Since Eqs. (25) and (2.11) have exactly the same form, we can write down the solution in a similar way:

$$\omega_p^2=[A(\mathbf{q})\omega_+^2-\omega_-^2]/[A(\mathbf{q})-1] \ , \tag{4.26}$$

where

$$A(\mathbf{q})=\exp[q\pi/mv_{1111}(\mathbf{q})] \ , \tag{4.27a}$$

$$\omega_\pm=q_xv_F\pm q_x^2/2m \ . \tag{4.27b}$$

We can also write the plasmon excitation equation of a 1D isolated superlattice in real space and use the wire index as a quantum number.[20] In the long-wavelength limit we have

$$\omega=(\omega_0 q_x a)\left[K_0(q_x a)+2\sum_{l=1}^{\infty}K_0(lqd)\cos(q_y ld)\right]^{1/2}, \tag{4.28}$$

where $\omega_0=(2N_w e^2/\epsilon m a^2)^{1/2}$. It is easy to prove that these two approaches are equivalent in the limit $a \ll d$.

In Fig. 6 we show the calculated intrasubband and intersubband excitations of a nontunneling quantum-wire superlattice as a function of $q_x$ for three different values of $q_y=0, 1/d, \pi/d$. The parameters used in our calculation are chosen according to the experimental data of Ref. 3 except that the linear density of electrons $N_w$ is taken to be $0.618\times10^5$ cm$^{-1}$ so as to be consistent with our assumption that only the lowest subband is occupied. As mentioned above, when $q_y$ is zero, the mode coupling vanishes. Comparing the three curves in Fig. 6, we conclude that the mode-coupling correction is small in our model, and, even for $q_y\neq0$, one can still talk about intrasubband and intersubband excitations as approximately separate entities without any significant error.

In the limit $q_x\rightarrow0$,

$$\Pi_{11}(q_x,\omega)=\frac{N_w}{m}\frac{q_x^2}{\omega^2}+O(q_x^4) \tag{4.29}$$

for nonzero $q_y$, $v_{1111}(q_x\rightarrow0,q_y)$ is finite, the intrasubband excitation energy goes to zero linearly as $q_x$ goes to zero; while for $q_y=0$, $v_{1111}(q_x\rightarrow0,q_y)$ diverges as $q_x^{-1}$ and the intrasubband excitation energy goes to zero as $q_x^{1/2}$, which is the expected long-wavelength behavior of the 2D plasmon dispersion. This is similar to the 2D superlattice situation, where for $q_z=0$ the plasmon dispersion in the long-wavelength limit goes to the 3D plasmon frequency.[44] In Fig. 6 the slope of the plasmon dispersion for small $q_x$ increases as $q_y$ decreases from $\pi/d$ to zero. At $q_y=0$, the slope diverges as $q_x^{-1/2}$. This differs from the single-quantum-wire case (cf. Sec. II), where the slope diverges as $|\ln(q_x a)|^{1/2}$. For large $q_x$, our calculation shows that the bandwidth of the plasmon excitation decreases as we increase $q_x$, i.e, the curves corresponding to different value of $q_y$ tend to merge as $q_x$ increases. From Fig. 6 we also see that the intersubband collective excitation is about 160–170 $\hbar^2/2ma^2$, that is, about 5.5 times larger than the corresponding single-particle excitation, which is $3\pi^2h^2/2ma^2$ for a square-well-type potential.

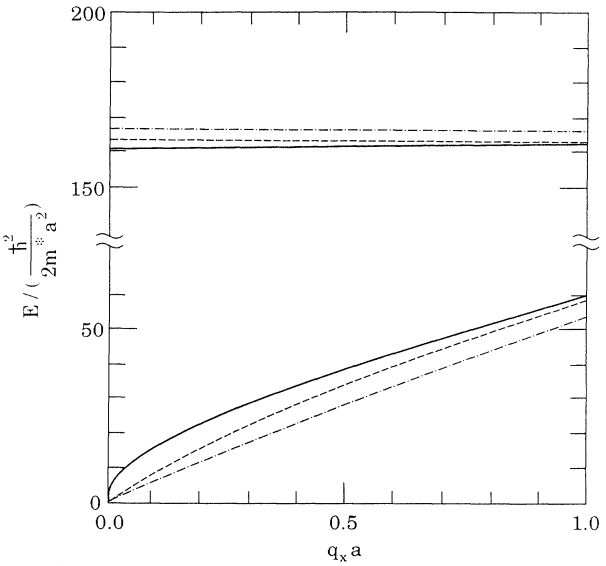


FIG. 6. The intrasubband (lower branch) and intersubband (upper branch) collective excitations of the nontunneling superlattice as a function of $q_x a$ for three different values of $q_y$: 0, $1/d$, and $\pi/d$ (solid, dashed, and dashed-dotted lines, respectively). The parameters are $a=550$ nm, $d=2a$, and $N_w=0.618\times10^5$ cm$^{-1}$.

This is in agreement with the recent experiment of Demel *et al.*,[3] who find that the intersubband collective excitation is 4 times larger than the corresponding single-particle excitation.

In Fig. 7 we show both the intrasubband and intersubband excitations as functions of $q_y$ at fixed $q_x=0.8/a$. The intrasubband excitation decreases,, while the intersubband excitation increases when we increase $q_y$ from 0 to $\pi/d$. Obviously, for a 1D superlattice with period $d$, one expects that the excitation should be a periodic function of $q_y$ with period $2\pi/d$ [cf. Eq. (19)].

### B. 1D superlattices with weak tunneling

Next we consider the 1D superlattice with weak tunneling. We only include the nearest-neighbor wave-function overlap. In this case, Eq. (12) can be written as

$$\begin{aligned}U_{nmn'm'}(q_x,k_y,q_y,k_y',q_y')&=\delta_{q_y,q_y'}U_{nmn'm'}(q_x,k_y,q_y,k_y')\\&=\delta_{q_y,q_y'}\frac{2\pi e^2}{\epsilon L}R_{nk_y}R_{mk_y+q_y}R_{n'k_y'}R_{m'k_y'+q_y}\\&\times\int dy\int dy'[u_n^*(y)u_m(y)+u_n^*(y+d)u_m(y)e^{ik_y d}+u_n^*(y-d)u_m(y)e^{-ik_y d}]\\&\times S(\mathbf{q},y-y')[u_{n'}(y')u_{m'}^*(y')+u_{n'}(y'+d)u_{m'}^*(y')e^{-ik_y' d}\\&+u_{n'}(y'-d)u_{m'}^*(y')e^{ik_y' d}]\,.\end{aligned} \tag{4.30}$$

Thus Eq. (11) becomes

$$\langle nk_y|V^H|mk_y+q_y\rangle=\sum_{n',m'}\sum_{k_y'}\Pi_{n'm'}(q_x,\omega,k_y',q_y')U_{nmn'm'}(q_x,k_y,q_y,k_y')\langle n'k_y'|V^{\rm ex}+V^H|m'k_y'+q_y\rangle \ . \tag{4.31}$$

The collective excitations of the system are given by the condition that Eq. (31) has nonzero solution $V^H$ when external perturbation $V^{\rm ex}$ is zero. In the following calculation we restrict ourselves to the lowest subband only, i.e., we only consider the case $m=n=m'=n'=1$. Then Eq. (31) can be simplified as

$$\langle k_y|V^H|k_y+q_y\rangle=\sum_{k_y'}\Pi(q_x,\omega,k_y',q_y')U(q_x,k_y,q_y,k_y')\langle n'k_y'|V^{ex}+V^H|m'k_y'+q_y'\rangle \ . \tag{4.32}$$

Here we have omitted the subband index subscripts, since all of them are equal to 1 under the assumption. In the linear-response regime it is sufficient to consider the response of the system to a perturbation in a single mode.[45] We write the induced Hartree potential as

$$V^H(y)=\sum_l v_l e^{i(q_y+2\pi l/d)y} \ . \tag{4.33}$$

Here we have omitted the dependence on $q_x$ and $\omega$ for simplicity. Thus we have

$$\langle k_y|V^H|k_y+q_y\rangle=\mathbf{b}(k_y,q_y)\cdot\mathbf{V}^H \ , \tag{4.34}$$

where $\mathbf{b}$ and $\mathbf{V}^H$ are three-dimensional vectors,

$$\mathbf{b}(k_y,q_y)=R_{1k_y}R_{1k_y+q_y}\times(1,\cos)k_yd),i\sin(k_yd)) \ , \tag{4.35}$$

and

$$(V^H)_i=\int dy\, f_i(y)V^H(y),\quad i=1,2,3 \ , \tag{4.36}$$

with

$$f_1(y)=u_1(y)u_1(y) \ , \tag{4.37a}$$

$$f_2(y)=u_1(y+d)u_1(y)+u_1(y-d)u_1(y) \ , \tag{4.37b}$$

$$f_3(y)=u_1(y+d)u_1(y)-u_1(y-d)u_1(y) \ . \tag{4.37c}$$

We define a $3\times3$ interaction matrix for the nearest-neighbor overlap case,

$$[\underline{W}(\mathbf{q})]_{ij}=\frac{2\pi e^2}{\epsilon L}\int dy\int dy' f_j(y)S(\mathbf{q},y-y')f_i(y') \ . \tag{4.38}$$

Then

$$U(q_x,k_y,q_y,k_y')=\mathbf{b}^\dagger(k_y',q_y)\cdot\underline{W}(\mathbf{q})\cdot\mathbf{b}(k_y,q_y) \ , \tag{4.39}$$

where $\mathbf{b}^\dagger$ is the Hermitian conjugate of $\mathbf{b}$. We also define a $3\times3$ polarizability matrix,

$$\underline{P}(\mathbf{q},\omega)=\sum_{k_y}\mathbf{b}(k_y,q_y)\Pi_{11}(q_x,\omega,k_y,q_y)\mathbf{b}^\dagger(k_y,q_y) \ . \tag{4.40}$$

Then at $V^{\rm ex}=0$, Eq. (32) can be rewritten as

$$\mathbf{V}^H\cdot[\underline{1}-\underline{W}(\mathbf{q})\cdot\underline{P}(\mathbf{q},\omega)]\cdot\mathbf{b}(k_y,q_y)=0 \ . \tag{4.41}$$

Here $\underline{1}$ is the $3\times3$ unit matrix. Equation (41) has nonzero solution $\mathbf{V}^H$ if and only if

$$\det|\underline{1}-\underline{W}(\mathbf{q})\cdot\underline{P}(\mathbf{q},\omega)|=0 \ . \tag{4.42}$$

This is the intrasubband plasmon excitation equation for the weak-tunneling 1D quantum-wire superlattice.

We solve Eq. (42) by expanding it in a Taylor series up to first order of $\alpha_1$ or $\Delta_1$. After some lengthy manipulations, we have

$$\det|\underline{1}-\underline{W}(\mathbf{q})\cdot\underline{P}(\mathbf{q},\omega)|=1-v(\mathbf{q})[\Pi_{11}(q_x,\omega)+c(q_x,\omega)\Delta_1]+O(\alpha^2)=0 \ , \tag{4.43}$$

where $\Pi_{11}$ and $\Delta_1$ are given by Eqs. (23) and (6), $v(\mathbf{q})$ is the Coulomb interaction matrix $v_{1111}(\mathbf{q})$ as given by Eq. (21), which can be further simplified as

$$v(\mathbf{q})=\sum_l[q_x^2+(q_y+2\pi l/d^2]^{-1/2}\times\left|\int dy\, u_1^2(y)e^{-i(q_y+2\pi l/d)y}\right|^2 \ , \tag{4.44}$$

and $c(q_x,\omega)$ is given by

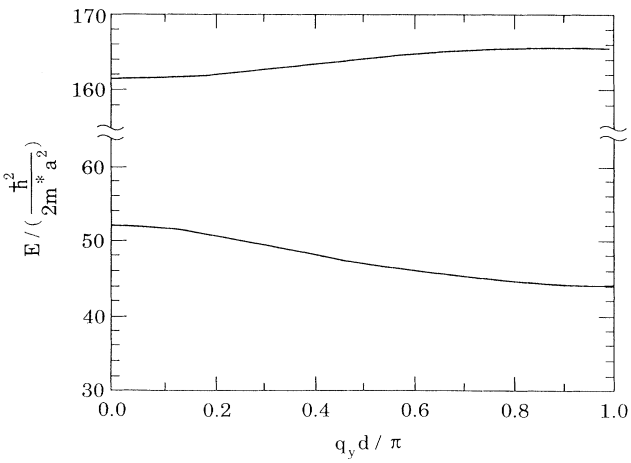


FIG. 7. The intrasubband (lower branch) and intersubband (upper branch) collective excitations of a nontunneling superlattice as a function of $q_y$ at a fixed $q_x=0.8/a$. The parameters are the same as in Fig. 6.

$$c(q_x,\omega)=\frac{m}{\pi k_F}\left[\frac{q_x v_F-E_q}{\omega^2-(q_x v_F-E_q)^2}-\frac{q_x v_F+E_q}{\omega^2-(q_x v_F+E_q)^2}\right]. \quad (4.45)$$

In Fig. 8 we show the intrasubband plasmon dispersion in the tunneling superlattice as a function of $q_x$ for three different values of $q_y$: 0, $1/d$, and $\pi/d$ at $V_0=100\hbar^2/2ma^2$. In this case, the overlap parameter [cf. Eq. (5)] $\alpha_1$ is $0.1\times10^{-4}$ and $\Delta_1$ [cf. Eq. (6)] is $6.0\times10^{-4}\ \hbar^2/2ma^2$; the higher-order terms are apparently negligible. For nonzero $q_y$, the plasmon energy goes to zero linearly as $q_x$ goes to zero, while for $q_y=0$, it goes to zero as $q_x^{1/2}$. Quantum tunneling does not change the dispersion power law, but modifies the coefficient in front of it. The coefficient becomes smaller as the tunneling gets stronger. In Fig. 9 we plot the plasmon excitation as a function of $q_x$ for four different values of $V_0=\infty$, 100, 20, and 5 (in units of $\hbar^2/2m^*a^2$) for a fixed $q_y=1/d$. The corresponding $\alpha_1$ increases from zero to 0.22 and $\Delta_1$ from zero to $1.15\hbar^2/2m^*a^2$. We can clearly see that when the barrier is lowered, i.e., the tunneling is increased (we keep $d=2a$ fixed), the plasmon excitation energy goes down. The reason for this is that for increased tunneling, the wave function spreads wider, which is equivalent to increasing the wire width $a$, consequently causing a lowering of the plasmon energy.[20] It should be noted that the above discussion is based on the assumption of a weak-tunneling limit. When tunneling gets strong enough so that we should include more than just the nearest-neighbor overlap, the whole picture may change.

Finally, we want to point out that Eqs. (11) and (12) are generally valid for calculating the plasmon excitations of a 1D superlattice. It works in the multisubband case and is not limited to nontunneling or nearest-neighbor overlapping superlattices only. The examples that we considered above are only the simplest applications of Eq. (11). With larger-scale numerical calculation, one can go further than that.

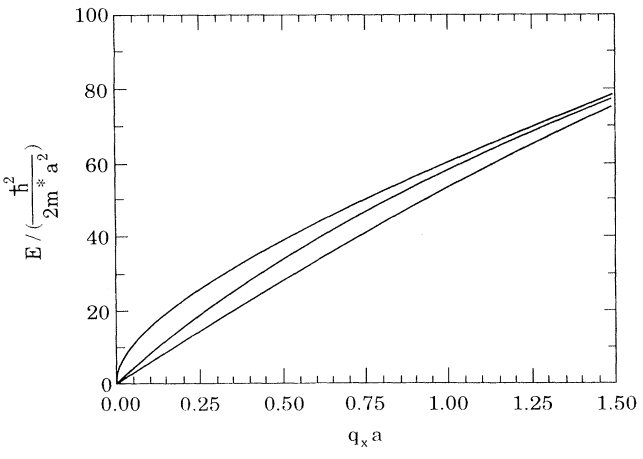


FIG. 8. The intrasubband plasmon excitation of a tunneling superlattice as a function of $q_x a$ for three different values of $q_y$, from the above: 0, $1/d$, and $\pi/d$. The barrier height $V_0$ is $100\hbar^2/2ma^2$, which corresponds to an overlap of $\alpha_1=0.11\times10^{-4}$. Other parameters are the same as in Fig. 6.

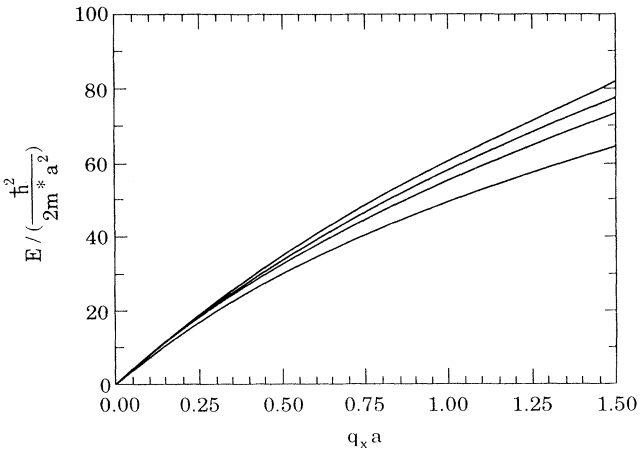


FIG. 9. The intrasubband plasmon excitation of a tunneling superlattice as a function of $q_x$ at a fixed $q_y=1/d$ for four different values of the barrier height $V_0$, from the above: $\infty$, 100, 50, and 5 (in unit of $\hbar^2/2ma^2$), which correspond to $\alpha_1=0$, $0.11\times10^{-4}$, $0.11\times10^{-1}$, and 0.22, respectively. Other parameters are the same as in Fig. 6.

## V. SPECTRAL WEIGHTS OF THE ELEMENTARY EXCITATIONS IN 1DES

In the previous sections, we have calculated the elementary excitation frequencies in various circumstances: single wire, multiple wires, and double-layered quantum wires. In all the calculations, we have calculated only the excitation energies, which correspond to the positions of the peaks in spectroscopic experiments. However, the light-absorption or Raman-scattering experiments do not only measure the position of the peak, but also the line shape of the peak, which, of course, contains some additional information of the system being probed. To have a complete comparison with experiments, we should also calculate the spectra weights. Theoretically, the calculation of the spectral weights (line shapes) is more involved than the determination of the plasmon energies, because the position of the peak is determined by the pole of the density-density correlation function (DDCF, also called the dynamical polarizability function, see Sec. II) and does not involve the full knowledge of the DDCF, whereas the spectral weight is proportional to the imaginary part of the dynamical polarizability function for Raman-scattering experiments and is proportional to the real part of the conductivity in light-absorption experiments. In Raman-scattering experiments (also called inelastic light scattering spectroscopy), one measures the imaginary part of the DDCF directly for finite wave vector $\mathbf{q}$. Since the Coulomb interaction is spin independent, i.e., it does not flip spins, the DDCF calculated without screening (single bare bubble) $D_{ij}^0$ corresponds to the

spin-density excitation, whereas the DDCF calculated with screening using the random-phase approximation $D_{ij,kl}$ corresponds to the charge-density (or collective) excitation.[38,46] In infrared-light-absorption experiments, we are always in the long-wavelength limit, since the speed of light is always much larger than the Fermi velocity in 1DES's, which is the slope of the single-particle dispersion relation. In order to increase the range of wave vectors that can be probed, one can use a grating coupler of period $d$ to allow jumps in the probed wave vector by $2\pi n/d$,[47,48] where $n$ is an integer.

The time-ordered density-density correlation function is defined in the usual way:

$$D(x,y,t;x',y',t')=-i\langle \mathcal{T}n(x,y,t)n(x',y',t')\rangle \ , \tag{5.1}$$

where we have assumed that the 1DES is confined in a zero-thickness $x$-$y$ plane and the $z$ coordinate is dropped. The quantity $n(x,y,t)$ is the electron density operator in the Heisenberg representation and $\mathcal{T}$ is the time-ordering operator. $D(x,y,t;x',y',t')$ depends on $x$ and $x'$ only through the difference $x-x'$ due to the translational symmetry in the $x$ direction, and, therefore, one can Fourier transform it in the variables $x-x'$ and $t-t'$ to get $D(q,\omega;y,y')$. We can expand $D(q,\omega;y,y')$ in terms of the wave function in the $y$ direction,[38]

$$D(q,\omega;y,y')=\sum_{i,j,k,l} D_{ij,kl}(q,\omega) \times\phi_i(y)\phi_j(y)\phi_k(y')\phi_l(y') \ . \tag{5.2}$$

Using the standard RPA treatment, $D_{ij,kl}$ is given by

$$D_{ij,kl}=D^0_{ij}\delta_{ik}\delta_{jl}+D^0_{ij}\sum_{m,n} V_{ijmn}D_{mn,kl} \ , \tag{5.3}$$

where $V_{ijmn}$ is the matrix element of the Coulomb interaction given by Eq. (1.6), and $D^0_{ij}$ is the density-density correlation function in the absence of Coulomb interactions,

$$D^0(q,\omega;y,y')=\sum_{i,j} D^0_{ij}(q,\omega)\phi_1(y)\phi_j(y)\phi_i(y')\phi_j(y') \ . \tag{5.4}$$

We use Matsubara's finite-temperature formula[41,42] to calculate $D^0_{ij}$,

$$\begin{aligned} D^0_{ij}(q,i\omega_n)&=\frac{2}{L\beta}\sum_p\sum_{p_n}\mathcal{G}^{(0)}_j(p+q,ip_n+i\omega_n) \times\mathcal{G}^{(0)}_i(p,ip_n) \\ &=\frac{2}{L}\sum_p\frac{f_F(E_j(p+q))-f_F(E_i(p))}{E_j(p+q)-E_i(p)-i\omega_n} \ , \end{aligned} \tag{5.5}$$

where $f_F(E_j(p+q))$ is the Fermi distribution function and $\omega_n=n2\pi/\beta$ is the complex frequency; $n$ is even for bosons and odd for fermions (here it is even), $\mathcal{G}^{(0)}_i(p,ip_n)$ is the Matsubara Green's function of the electrons in the $i$th subband in the absence of the Coulomb interaction $p\equiv p_x$, $q\equiv q_x$, and $\beta\equiv 1/k_BT$. To calculate the Raman-scattering intensity, one replaces the complex frequency $i\omega_n$ by $\omega+i\gamma$. But this simple replacement violates the conservation of the number of particles. Instead, we should use the correct form of $D^0$, suggested by Mermin,[49] which is

$$D^0\rightarrow\frac{D^0(q,\omega+i\gamma)(1+i\gamma/\omega)}{1+i(\gamma/\omega)D^0(q,\omega+i\gamma)/D^0(q,0)} \ .$$

Making this correction does not lead to any significant changes in our result. To simplify the notation, we still use the simple replacement of $i\omega_n$ by $\omega+i\gamma$. Here $\gamma$ is the phenomenological parameter characterizing the broadening of energy levels due to the impurities and imperfections. From Eq. (6), we get

$$D^0_{ij}=\frac{1}{\pi}\int dk\left[\frac{f_F(E_j+k^2/2m)}{E_{ji}+k^2/2m-(k-q)^2/2m-(\omega+i\gamma)}-\frac{f_F(E_i+k^2/2m)}{E_{ji}+(k+q)^2/2m-k^2/2m-(\omega+i\gamma)}\right] . \tag{5.6}$$

In the $\gamma\rightarrow 0$ limit,

$$\begin{aligned} \mathrm{Im}D^0_{ij}(q,\omega)&=\frac{1}{\pi}\int dk\left[\frac{\pi\delta(\omega-E_{ji}-kq/m+q^2/2m)}{\exp[\beta(E_j+k^2/2m-\mu)]+1}-\frac{\pi\delta(\omega-E_{ji}-kq/m-q^2/2m)}{\exp[\beta(E_i+k^2/2m-\mu)]+1}\right] \\ &=\frac{m}{q}\left[\frac{1}{\exp[\beta(E_j+k_1^2/2m-\mu)]+1}-\frac{1}{\exp[\beta(E_i+k_2^2/2m-\mu)]+1}\right] . \end{aligned} \tag{5.7}$$

Here

$$k_1=\frac{m}{q}(\omega-E_{ji}+q^2/2m) \ , \tag{5.8a}$$

$$k_2=\frac{m}{q}(\omega-E_{ji}-q^2/2m) \ , \tag{5.8b}$$

where $E_{ji}\equiv E_j-E_i$ is the energy separation of the $j$th and $i$th subbands, and $\mu$ the chemical potential.

First we consider a single quantum wire and assume the two-subband model (see Sec. II). From Eq. (4) we have

$$\begin{aligned} D^0(q_x,\omega,q_y)&=\int dy\int dy_1 e^{-iq_y(y-y_1)} \times D^0(q_x,\omega;y,y_1) \\ &=\sum_{i,j} D^0_{ij}(q_x,\omega)C_{ij}(q_y) \ , \end{aligned} \tag{5.9a}$$

with

$$C_{ij}(q_y)=\int dy \int dy_1 \phi_i(y)\phi_j(y)e^{-iq_y(y-y_1)} \times \phi_i(y_1)\phi_j(y_1) \ . \tag{5.9b}$$

We assume that the confinement potential in the $y$ direction is the square-well type with well width $a$. In this case, $C_{ij}$ is calculated to be

$$C_{11}(q_y)=2[1-\cos(q_y a)] \times \left[ \frac{1}{(q_y a)^2}+\frac{28\pi^2-5q_y^2a^2}{2(4\pi^2-q_y^2a^2)^2} \right] , \tag{5.10a}$$

$$C_{12}(q_y)=C_{21}(q_y) =2[1+\cos(q_y a)] \times \left[ \frac{81\pi^2-5q_y^2a^2}{4(9\pi^2-q_y^2a^2)^2}-\frac{\pi^2-5q_y^2a^2}{4(\pi^2-q_y^2a^2)^2} \right] . \tag{5.10b}$$

In the two-subband model, we assume only the lowest subband to be occupied. At zero temperature, $D_{22}^0$ is zero. For finite temperature, as long as $k_B T \ll E_{21}$ (more precisely, $k_B T \ll E_2-\mu$, where $\mu$ is the chemical potential), we can still neglect $D_{22}^0$. Thus

$$D^0(q_x,\omega,q_y)=\sum_{i,j} D_{ij}^0(q_x,\omega)C_{ij}(q_y) =C_{11}D_{11}^0+C_{12}(D_{12}^0+D_{21}^0) \ . \tag{5.11}$$

The Raman-scattering intensity is proportional to the imaginary part of $D^0(q_x,\omega,q_y)$. Since $C_{ij}$ is real, we get

$$\mathrm{Im}D^0(q_x,\omega,q_y)=C_{11}(\mathrm{Im}D_{11}^0) +C_{12}(\mathrm{Im}D_{12}^0+\mathrm{Im}D_{21}^0) \ . \tag{5.12}$$

In Fig. 10 we show, in the limit of $\gamma \to 0$ [cf. Eq. (7)] the calculated Raman-scattering intensity of the spin-density (single-particle) excitation of a 1DES with the 1D electron density $N_w=0.888\times10^5$ cm$^{-1}$, $a=390$ nm at fixed $q_x=1/a$ and $T=0.33E_{21}/k_B$ for three different values of $q_y=1/a$, $2/a$, and $4/a$ [Figs. 10(a), 10(b), and 10(c)], respectively. We can see clearly that as $q_y$ is increased, the spectral weight of the intersubband excitation increases.

The calculation of the Raman-scattering intensity of the collective excitation is more complicated. In the two-subband model we can solve Eq. (3):

$$D_{1111}=\frac{(1-D_{22}^0V_{2222})D_{11}^0}{(1-D_{11}^0V_{1111})(1-D_{22}^0V_{2222})-D_{11}^0D_{22}^0(V_{1122})^2} , \tag{5.13a}$$

$$D_{1211}=D_{2111}=D_{1112}=D_{1121}=D_{1222}=D_{2122}=D_{2212}=D_{2221}=0 , \tag{5.13b}$$

$$D_{1122}=D_{2211}=\frac{D_{22}^0V_{1122}D_{11}^0}{(1-D_{11}^0V_{1111})(1-D_{22}^0V_{2222})-D_{11}^0D_{22}^0(V_{1122})^2} , \tag{5.13c}$$

$$D_{2222}=\frac{(1-D_{11}^0V_{1111})D_{22}^0}{(1-D_{11}^0V_{1111})(1-D_{22}^0V_{2222})-D_{11}^0D_{22}^0(V_{1122})^2} , \tag{5.13d}$$

$$D_{1212}=\frac{(1-D_{21}^0V_{1212})D_{12}^0}{1-(D_{12}^0+D_{21}^0)V_{1212}} , \tag{5.13e}$$

$$D_{2121}=\frac{(1-D_{12}^0V_{1212})D_{21}^0}{1-(D_{12}^0+D_{21}^0)V_{1212}} , \tag{5.13f}$$

$$D_{2112}=D_{1221}=\frac{D_{21}^0V_{1212}D_{12}^0}{1-(D_{12}^0+D_{21}^0)V_{1212}} . \tag{5.13g}$$

In the low-temperature limit $\beta(E_2-\mu)\gg1$, $D_{22}^0$ goes to zero in the two-subband model. Thus

$$D_{1111}=\frac{D_{11}^0}{1-D_{11}^0V_{1111}} , \tag{5.14a}$$

$$D_{1212}=\frac{(1-D_{21}^0V_{1212})D_{12}^0}{1-(D_{12}^0+D_{21}^0)V_{1212}} , \tag{5.14b}$$

$$D_{2121}=\frac{(1-D_{12}^0V_{1212})D_{21}^0}{1-(D_{12}^0+D_{21}^0)V_{1212}} , \tag{5.14c}$$

$$D_{2112}=D_{1221}=\frac{D_{21}^0V_{1212}D_{12}^0}{1-(D_{12}^0+D_{21}^0)V_{1212}} , \tag{5.14d}$$

$$D_{1122}=D_{2211}=D_{2222}=0 . \tag{5.14e}$$

The pole of the $D_{1111}$, which is

$$1-D_{11}^0V_{1111}=0 , \tag{5.15}$$

determines the intrasubband plasmon excitation; and the

pole of $D_{1212}$ (or $D_{2121}, D_{2112}, D_{1221}$), which is

$$1-(D_{12}^0+D_{21}^0)V_{1212}=0 , \tag{5.16}$$

determines the intersubband collective excitation. This is exactly what we get in Sec. II (note that $D_{ij}^0 \equiv \Pi_{ij}$) for the two-subband model.

Similar to the spin-density excitation [Eq. (9)], we Fourier transform Eq. (2) for the charge-density excitation and get

$$D(q_x,\omega,q_y)=\int dy \int dy_1 e^{-iq_y(y-y_1)} D(q_x,\omega;y,y_1)$$
$$=\sum_{i,j,k,l} D_{ijkl}(q_x,\omega)B_{ijkl}(q_y) , \tag{5.17a}$$

with

$$B_{ijkl}(q_y)=\int dy \int dy_1 \phi_i(u)\phi_j(y) \times e^{-iq_y(y-y_1)}\phi_k(y_1)\phi_l(y_1) . \tag{5.17b}$$

Substituting Eqs. (14) and (13b) into Eq. (17a), we get

$$D(q_x,\omega,q_y)=B_{1111}D_{1111}+B_{1212}(D_{1212}+D_{2112}+D_{1221}+D_{2121})$$
$$=B_{1111}\frac{D_{11}^0}{1-D_{11}^0V_{1111}}+B_{1212}\frac{D_{21}^0+D_{12}^0}{1-(D_{12}^0+D_{21}^0)V_{1212}} . \tag{5.18}$$

Comparing Eqs. (17b) and (9b) yields

$$B_{1111}=C_{11}, \quad B_{1212}=C_{12} . \tag{5.19}$$

The values of $C_{11}$ and $C_{12}$ in a square-well-type potential are given by Eq. (10). We can see clearly from Eq. (18) that in the two-subband model the Raman-scattering intensity is the sum of two parts: intrasubband and intersubband plasmon excitations.

In Fig. 11 we show the Raman-scattering intensity of the charge-density excitations for the 1DES with $N_W=0.888\times10^5$ cm$^{-1}$, $\alpha=390$nm, $\gamma=\hbar^2/2ma^2$ at fixed $q_x=1/a$ and $T=0.10E_{21}/k_B$ for three different values of $q_y=1/a$, $2/a$, and $4/a$ [Figs. 11(a), 11(b), and 11(c)], respectively. In the numerical calculation we have actually included the second subband completely, i.e., we use Eq. (13) instead of the low-temperature-limit form [Eq. (14)].

In Fig. 12 we show the Raman-scattering intensity of the charge-density excitation at fixed $q_y=4/a$ for the same system as in Fig. 11 except $\gamma=5.0\hbar^2/2ma^2$ [Fig. 12(a)] and $\gamma=10.0\hbar^2/2ma^2$ [Fig. 12(b)]. The half-widths of the peaks are determined by $\gamma$ and the temperature $T$.

Next we consider the case of a 1D quantum-wire superlattice; we restrict ourselves to the case of isolated 1D superlattices (see Sec. IV). For the spin-density excitations, the Raman-scattering intensity of the 1D superlattice is nothing but the sum of the contributions of each individual quantum wire, since it is calculated in the absence of the Coulomb interaction, and is, therefore enhanced by a factor of $N$, which is the number of quantum wires in the superlattice. The relative profile (or line shape) does not change. For the charge-density excitations, the Raman-scattering intensity of the 1D superlattice can be calculated by replacing the Coulomb interaction matrix elements of a single wire [Eq. (1.5)],

$$v(q,y-y')=(2e^2/\epsilon)K_0(|q(y-y')|) \tag{5.20a}$$

by the Coulomb interaction matrix elements of the 1D quantum-wire superlattice [Eq. (4.19)],

$$S(\mathbf{q},y-y')=\sum_s \frac{\exp[-i(q_y+s2\pi/d)(y-y')]}{[q_x^2+(q_y+s2\pi/d)^2]^{1/2}} , \tag{5.20b}$$

where the summation is over all integers $s$.

It turns out that the matrix elements of Coulomb interaction in the 1D isolated superlattices can be calculated explicitly for the square-well-type potential, considerably simplifying the numerical calculation of the spectral weight. For example,

$$V_{1111}(\mathbf{q})=\int dy \int dy_1 u_1(y)u_1(y)S(\mathbf{q},y-y_1)u_1(y_1)u_1(y_1)$$
$$=\sum_s \frac{2\sin[(q_y+s2\pi/d)a/2]}{[q_x^2+(q_y+s2\pi/d)^2]^{1/2}}\left[\frac{1}{q_y+2\pi s/d}-\frac{q_y+2\pi s/d}{(q_y+2\pi s/d)^2-(2\pi/a)^2}\right] . \tag{5.21}$$

In Fig. 13 we show the calculated spectral weights of the charge-density excitations in the 1D quantum-wire superlattices (no tunneling) with $N_w=0.872\times10^6$ cm$^{-1}$, $\alpha=39$ nm, $\gamma=\hbar^2/2ma^2=0.377$ meV, superlattice period $d=2a$, $q_x=q_y=1/a$ at temperature $T=0.44$ K [Fig. 13(a)] and $T=4.4$ K [Fig. 13(b)] respectively. In Fig. 13(b) the small peak on the left side is the intrasubband plasmon excitation of the second subband. In low temperature [Fig. 13(a)], the second subband is not populated, and its intrasubband plasmon excitation spectral weight is negligible.

In Fig. 14, we show the Raman-scattering intensity of

the charge-density excitations of the 1D quantum-wire superlattice with the same parameters as in Fig. 13(b) except for $\gamma=2\hbar^2/2ma^2$ [Fig. 14(a)] and $5\hbar/2ma^2$ [Fig. 14(b)], respectively. In Fig. 15 we show the Raman-scattering intensity of the charge-density excitations of the 1D quantum-wire superlattice with the same parameters as Fig. 13(b) except for $q_y=4.0/a$ [Fig. 15(a)] and $2.0/a$ [Fig. 15(b)], respectively. The peak on the left side (lower energy) is the intrasubband plasmon excitation and the peak on the right side is the intersubband collective

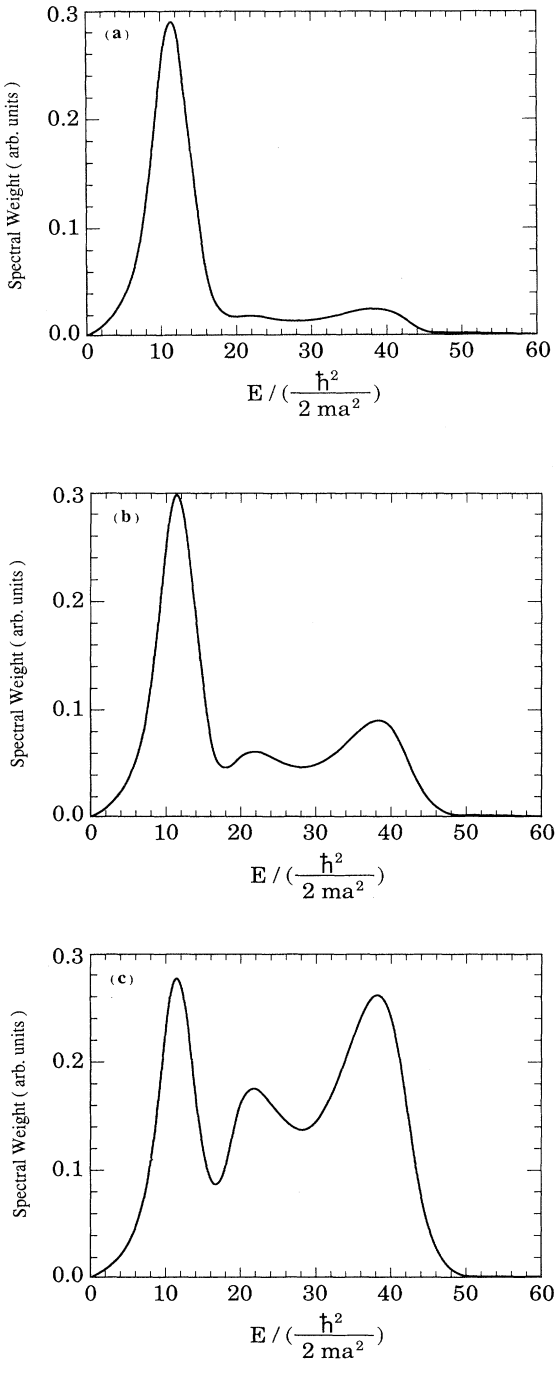


FIG. 10. The calculated Raman-scattering intensity of the spin-density excitation of a 1DES with $a=390$ nm, $N_w=0.885\times10^5$ cm$^{-1}$, and $\gamma\to0$ at fixed $q_x=1/a$ and $T=0.33E_{21}/k_B$ for three different values of $q_y=1/a$, $2/a$, and $4/a$ [(a), (b), and (c), respectively].

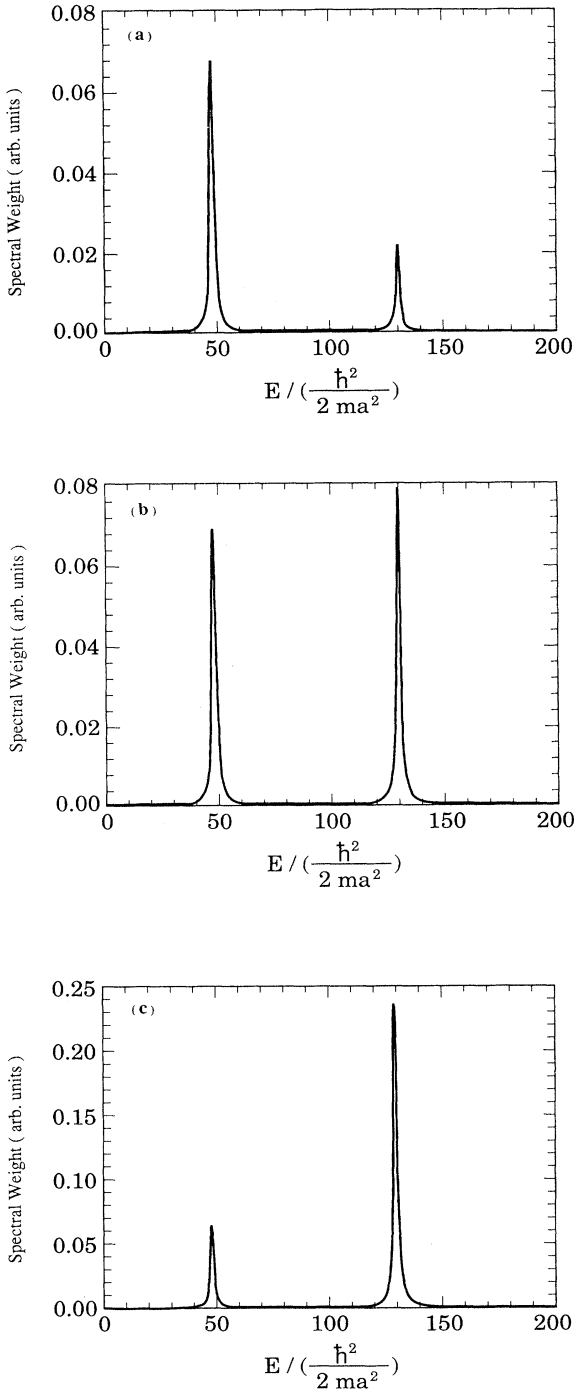


FIG. 11. The calculated Raman-scattering intensity of the charge-density excitation for three different values of $q_y=1/a$, $2/a$, and $4/a$ [(a), (b), and (c), respectively]. The parameters are the same as in Fig. 10 except $\gamma=\hbar^2/2ma^2$ and $T=0.1E_{21}/k_B$.

excitation. We can clearly see that as $q_y$ increases, the spectral weight of the intersubband plasmon excitation increases.

## VI. CONCLUSION

In this paper we have studied the elementary excitations in various quasi-one-dimensional electron systems in the zero magnetic field. We summarize our results and discuss the possible future directions of development in the field. Results of the elementary excitations in quantum wires in the presence of an external magnetic field will be published in another paper.[36]

In Sec. II, we studied the elementary excitations in a single quantum wire. The collective excitation energies were calculated explicitly for the two-subband and three-subband models under the random-phase approximation. We have included the mode-coupling effect between the intrasubband and intersubband excitations in our calculation. We find that the intersubband collective excitation frequency can be 5–6.5 times higher than the corresponding single-particle excitation energy due to a large depolarization shift in quasi-one-dimensional electron systems. This is in good agreement with the recent far-infrared spectroscopic experimental results.

In Sec. III, we calculated the plasmon excitation energy of a double-layered quantum-wire system. We find that because of the Coulomb interaction between the electrons in different layers, the 1D intrasubband plasmon frequency splits into two branches. One goes to zero as $q|\ln(qa)|^{1/2}$, while the other goes to zero linearly on $q$ in the long-wavelength limit. The intersubband collective excitation also exhibits a similar splitting.

We studied the elementary excitations in multiwire systems (or 1D lateral quantum-wire superlattices) in Sec. IV. We started from the linear-response theory and included the Coulomb interaction and the tunneling between neighboring wires. In the case of nontunneling superlattices, the equation determining the collective excitation energies is very similar to that of the single-wire

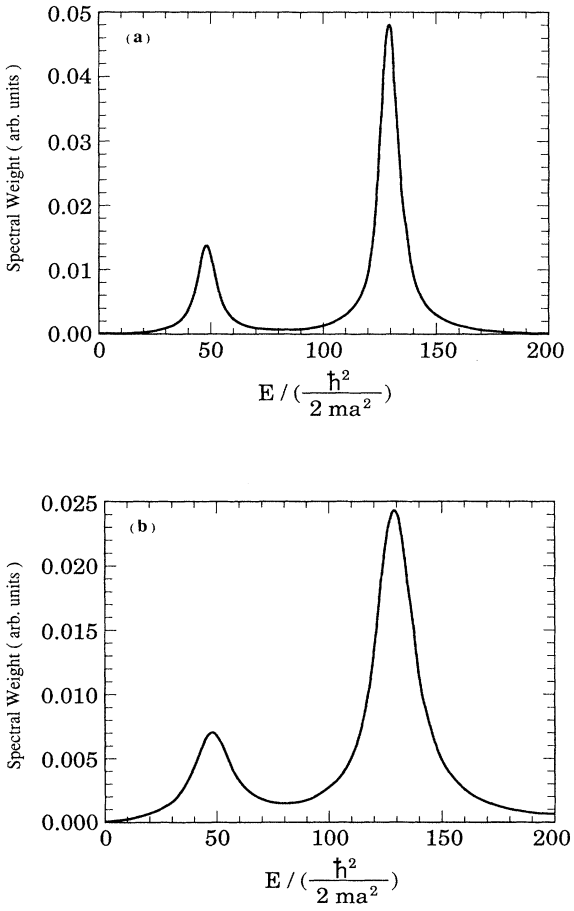


FIG. 12. The calculated Raman-scattering intensity of the charge-density excitation at fixed $q_y=4/a$ for the same parameters as in Fig. 11 except for $\gamma=5.0\hbar^2/2ma^2$ (a) and $10.0\hbar^2/2ma^2$).

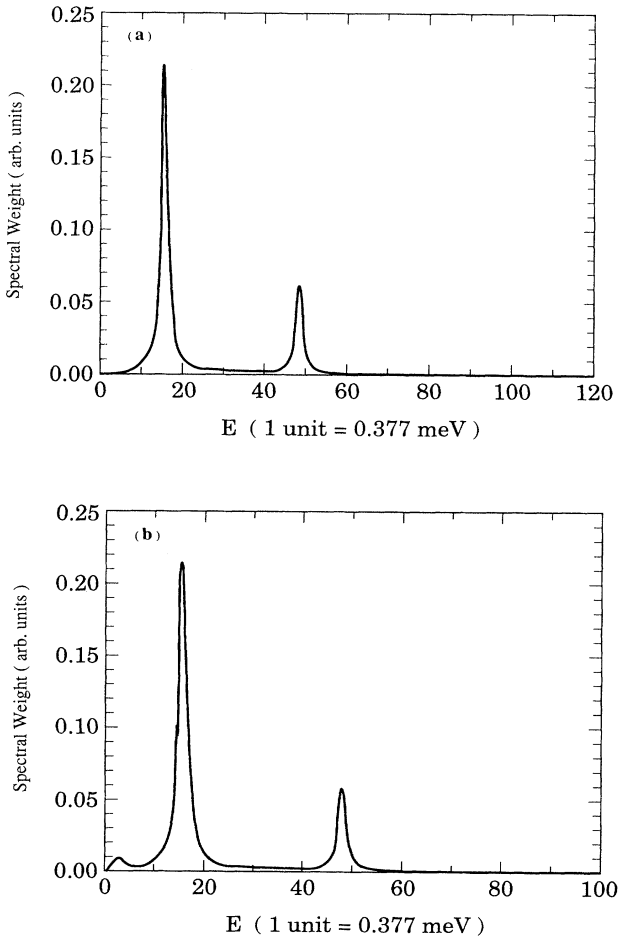


FIG. 13. The calculated Raman-scattering intensity of the charge-density excitations in a 1D quantum-wire superlattice with $a=39$ nm, $N_w=0.872\times10^6$ cm$^{-1}$, $\gamma=0.377$ meV, superlattice period $d=2a$, $q_x=q_y=1/a$ at temperature $T=0.44$ K and 4.4 K (b).

case, whereas the equation is more complicated in the case of tunneling superlattices. In the weak-tunneling limit, the intrasubband excitation energy decreases as the tunneling increases. For nonzero $q_y$ (where the $y$ direction is the direction of the superlattice and the $x$ direction is the free direction), the plasmon energy goes to zero linearly as $q_x$ goes to zero, while for $q_y=0$, it goes to zero as $q_x^{1/2}$. At least from the perturbation theory point of view, quantum tunneling does not change the dispersion power law, but only modifies the coefficient in front of it. The coefficient becomes smaller as tunneling gets stronger.

In Sec. V we calculated the spectral weights of the elementary excitations of the single quantum wire and the quantum-wire superlattice under the two-subband assumption. The Raman-scattering intensity is proportional to the imaginary part of the density-density correlation function. We calculated the density-density correlation function for two cases: with and without Coulomb interaction, which corresponds to the charge-density and spin-density excitations, respectively. We plot the Raman-scattering intensity for various parameter values including the temperature, the wave vector, and the impurity broadening width. The spectral weight of the intersubband excitation increases as $q_y$ increases.

Several important problems remain open. First, we use the RPA rather uncritically, based mainly on the fact that we do not know how to go beyond the RPA in a controlled approximation. The validity of the RPA in the 1D electron systems of interest here is unknown, but it is expected to be less valid than in higher dimensions. In some sense it is a surprise that our theory agrees so well with experiments. One possible reason may be that in GaAs systems the dimensionless ratio $r_s=r_0/a_0$ is rather small. Here $r_0$ is the average distance between electrons and $a_0=\epsilon\hbar^2/me^2$ is the Bohr radius. In the small $r_s$ limit, the kinetic energy of the electron system is much larger than its interaction energy, and the RPA is expected to be a good approximation. Second, our use of a model confinement in the RPA calculation can and

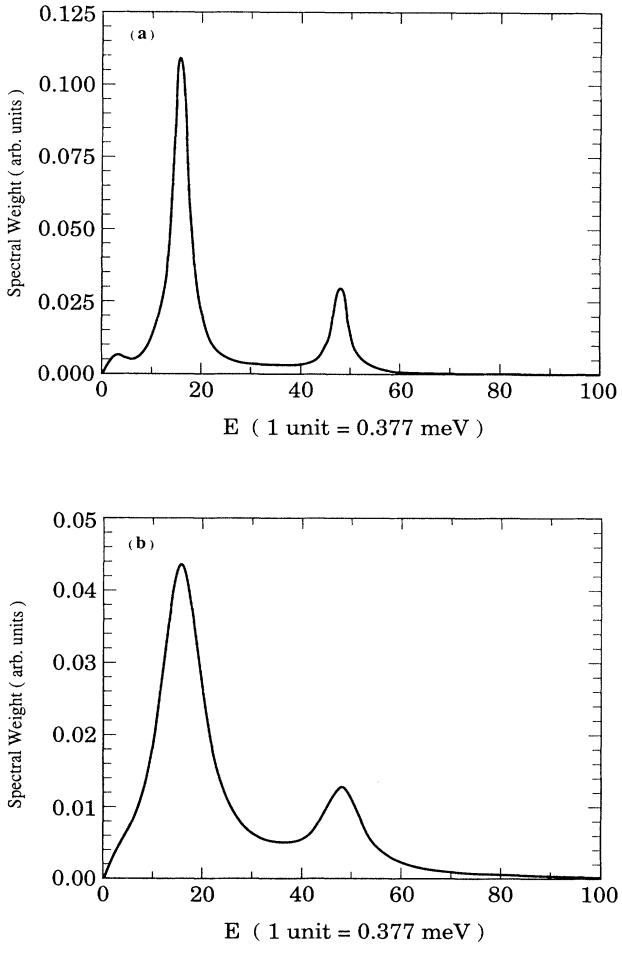


FIG. 14. The Raman-scattering intensity of the charge-density excitations of the 1D quantum-wire superlattice with the same parameters as Fig. 13(b) except for $\gamma=0.754$ meV and 1.885 meV (b).

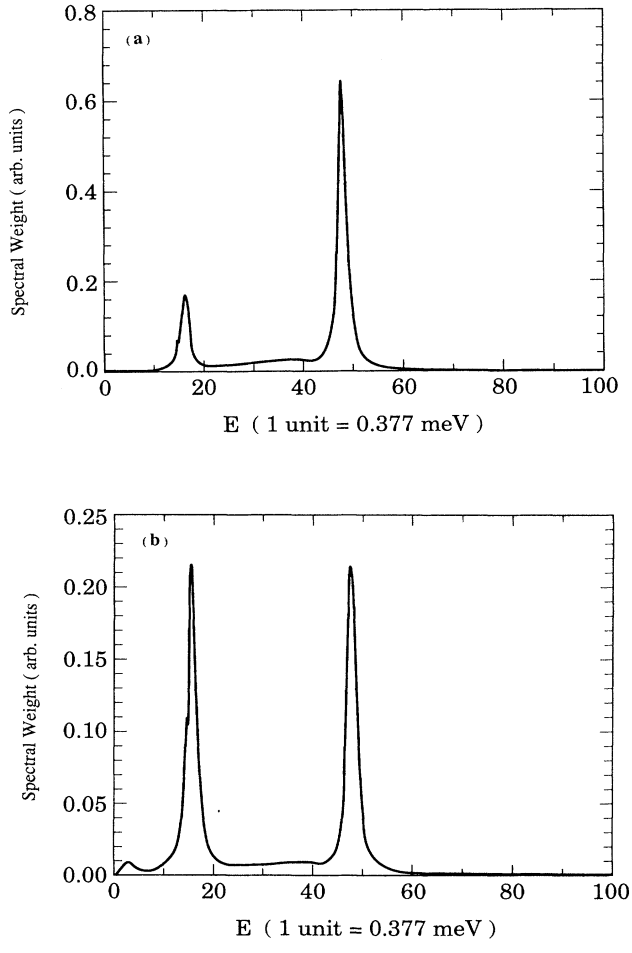


FIG. 15. Shows the Raman-scattering intensity of the charge-density excitations of the 1D quantum-wire superlattice. The parameters are the same as Fig. 13(b) except for $q_y=4/a$ (a) and $2/a$ (b), respectively.

should be improved in subsequent calculations in a more realistic self-consistent manner.[28] Finally, our calculations in this paper are based mostly on the two-subband and three-subband models. It is very hard to include a lot of subband using our method. To have a qualitative comparison between the theory and experiments, it is hoped that more experimental results in samples with fewer occupied subbands (ideally only one or two) will appear. We do not see any fundamental difficulties preventing one from doing that. To have such a qualitative comparison, it is also important that the confining potentials of the 1DES's be made in a more controllable manner, as in the 2DEG case. The direct MBE growth method to fabricate 1DES's seems to be a promising step in this direction. By carefully controlling the concentrations of different ingredients (such as Al and As in $Ga_{1-x}Al_xAs$ devices) in the growth process, one can tailor the band structure to achieve the confining potential as desired. This method has been successful in fabricating parabolic quantum-well samples.[50]

## ACKNOWLEDGMENTS

This work was supported by the U. S. Office of Naval Research (US-ONR) and the U. S. Army Research Office (US-ARO). We also acknowledge support from the University of Maryland Computer Center and the National Center for Supercomputing Applications at the University of Illinois at Urbana-Champaign.

*Present address: Department of Physics, University of Wisconsin, Madison, WI 53706.

[1]T. Ando, A. B. Fowler, and F. Stern, Rev. Mod. Phys. **54**, 437 (1982).
[2]W. Hansen, M. Horst, J. P. Kotthaus, U. Merkt, Ch. Sikorski, and K. Ploog, Phys. Rev. Lett. **58**, 2586 (1987).
[3]T. Demel, D. Heitmann, P. Grambow, and K. Ploog, Phys. Rev. B **38**, 12 732 (1988).
[4]J. H. F. Scott-Thomas, S. B. Field, M. A. Kastner, H. I. Smith, and D. A. Antoniadis, Phys. Rev. Lett. **62**, 583 (1989).
[5]P. M. Petroff, J. Gaines, M. Tsuchiya, R. Simes, L. Coldren, H. Kroemer, J. English, and A. C. Gossard, J. Cryst. Growth **95**, 260 (1989).
[6]S. He and S. Das Sarma, Phys. Rev. B **40**, 3379 (1989).
[7]P. A. Lee, A. D. Stone, and H. Fukuyama, Phys. Rev. B **35**, 1039 (1987).
[8]B. J. Van Wees *et al.*, Phys. Rev. Lett. **60**, 848 (1988).
[9]D. A. Wharam *et al.*, J. Phys. C **21**, L209 (1988).
[10]A. Szafer and A. D. Stone, Phys. Rev. Lett. **62**, 300 (1989).
[11]R. Landauer, Philos. Mag. **21**, 863 (1970).
[12]D. Weiss, K. von Klitzing, K. Ploog, and G. Weimann, Europhys. Lett. **8**, 179 (1989); R. R. Gerhardts, D. Weiss, and K. von Klitzing, Phys. Rev. Lett. **62**, 1173 (1989).
[13]R. W. Winkler, J. P. Kotthaus, and K. Ploog, Phys. Rev. Lett. **62**, 1177 (1989).
[14]P. Vasilopouslos and F. M. Peeters, Phys. Rev. Lett. **63**, 2120 (1989).
[15]H. L. Cui, V. Fessatidis, and N. J. M. Horing, Phys. Rev. Lett **63**, 2598 (1989).
[16]M. Büttiker, Phys. Rev. Lett. **57**, 1761 (1986).
[17]A. H. MacDonald, Phys. Rev. Lett. **64**, 220 (1990).
[18]T. Martin and S. Feng, Phys. Rev. Lett. **64**, 1971 (1990).
[19]X. C. Xie, Q. P. Li, and S. Das Sarma, Phys. Rev. B **42**, 7132 (1990).
[20]S. Das Sarma and W. Y. Lai, Phys. Rev. B **32**, 1401 (1985).
[21]Q. Li and S. Das Sarma, Phys. Rev. B **40**, 5860 (1989).
[22]J. Hubbard, Proc. R. Soc. London Ser. A **276**, (1963).
[23]E. H. Lieb and F. Y. Wu, Phys. Rev. Lett. **20**, 1445 (1968).
[24]L. D. Landau, J. Phys. (Moscow) **10**, 25 (1946).
[25]D. Pines and P. Nozières, *The Theory of Quantum Liquids* (Benjamin, New York, 1966).
[26]W. Y. Lai and S. Das Sarma, Phys. Rev. B **33**, 8874 (1986); W. Y. Lai, A. Kobayashi, and S. Das Sarma, *ibid.* **34**, 7380 (1986).
[27]W. M. Que and G. Kirczenow, Phys. Rev. B **37**, 7153 (1988).
[28]S. Laux, D. Frank, and F. Stern, Surf. Sci. **196**, 101 (1988).
[29]T. P. Smith III, J. A. Brum, J. M. Hong, C. M. Knoedler, H. Arnot, and L. Esaki, Phys. Rev. Lett. **61**, 585 (1988).
[30]B. S. Mendoza and Y. C. Lee, Phys. Rev. B **40**, 12 063 (1989).
[31]H. L. Zhao, Y. Zhu, and S. Feng, Phys. Rev. B **40**, 8107 (1989).
[32]H. L. Cui, X. J. Lu, N. J. M. Horing, and X. L. Lei, Phys. Rev. B **40**, 3443 (1989); H. L. Cui and N. J. M. Horing, *ibid.* **40**, 2956 (1989).
[33]Q. Li and S. Das Sarma, Phys. Rev. B **41**, 10 268 (1990).
[34]G. Gumbs, D. Heitmann, and T. Demel (unpublished).
[35]H. Ehrenreich and M. Cohen, Phys. Rev. **115**, 786 (1959).
[36]Q. P. Li and S. Das Sarma (unpublished).
[37]S. Das Sarma, Phys. Rev. B **29**, 2334 (1984).
[38]J. K. Jain and S. Das Sarma, Phys. Rev. B **36**, 5949 (1987).
[39]S. J. Allen, D. C. Tsui, and B. Vinter, Solid State Commun. **20**, 425 (1976).
[40]S. Das Sarma and A. Madhukar, Phys. Rev. B **23**, 805 (1981).
[41]A. L. Fetter and J. D. Walecka, *Quantum Theory of Many-Particle Systems* (McGraw-Hill, New York, 1971).
[42]G. Mahan, *Many Particle Physics* (Plenum, New York, 1981).
[43]D. Yoshioka, B. I. Halperin, and P. A. Lee, Phys. Rev. Lett. **50**, 1219 (1983).
[44]S. Das Sarma and J. J. Quinn, Phys. Rev. B **25**, 7603 (1982).
[45]X. Zhu, X. Xia, J. J. Quinn,and P. Hawrylak, Phys. Rev. B **38**, 5617 (1988).
[46]S. Das Sarma, in *NATO Advanced Research Workshop on Light Scattering in Semiconductor Structures and Superlattices,* edited by D. J. Lockwood and J. F. Young (Plenum, New York, in press).
[47]L. Zheng, W. L. Schaich, and A. H. MacDonald, Phys. Rev. B **41**, 8493 (1990).
[48]T. N. Theis, Ph.D. thesis, Brown University, 1978.
[49]N. D. Mermin, Phys. Rev. B **1**, 2362 (1970).
[50]K. Karrai, H. D. Drew, M. W. Lee, and M. Shayegan, Phys. Rev. B **39**, 1426 (1989); K. Karrai, X. Ying, H. D. Drew, and M. Shayegan, *ibid.* **40**, 12 020 (1989).